

*Crystal Growth
from
High-Temperature
Solutions*

D. Elwell and H. J. Scheel

Online-Edition of the original book
with additional Chapter II and Appendices A and B



Academic Press London New York San Francisco

A subsidiary of Harcourt Brace Jovanovich, Publishers

Part 007

Please get the complete edition from
<http://e-collection.library.ethz.ch/view/eth:4822>

2011 © D. Elwell & H. J. Scheel

4. Theory of Solution Growth

4.1. Limitations of a Theoretical Treatment	138
4.2. Nucleation	139
4.3. Rough and Smooth Interfaces	143
4.4. Models of Surface Roughness	145
4.5. Stages in Growth from Solution	148
4.6. The Boundary Layer	151
4.7. Generation of Surface Steps	156
4.8. The Theory of Burton, Cabrera and Frank	160
4.9. Should Surface Diffusion be Included?	166
4.10. The Role of Desolvation	170
4.11. Comparison of Solution Growth Theory with Experiment	171
4.12. Non-Archimedean Spirals	176
4.13. Surface Morphology of Flux-grown Crystals	183
4.14. Alternative Growth Mechanisms	189
4.15. Summary	197
References	198

4.1. Limitations of a Theoretical Treatment

In this chapter we discuss those aspects of the theory of crystal growth from solution which relate to the growth mechanism. Reference is made where possible to experiments either on high-temperature or on aqueous solutions which support the various postulates introduced in the theory. A recent review of crystal-growth theory has been given by Parker (1970) and theoretical aspects of crystal growth from solution have also been reviewed by Bennema (1965), Khamskii (1969), Strickland-Constable (1968) and Lewis (1974).

Although the number of theoretical publications is quite extensive, reliable quantitative estimates of the growth rate under specified conditions still cannot be given for growth from solution. All the expressions for this most important parameter contain factors which cannot be assigned numerical values based on experiment. Any numerical estimates given therefore contain values which are crude approximations and so predictions from the theory are at best reliable only to the order of magnitude.

Another serious limitation mentioned in the previous chapter is that our present knowledge of the detailed atomic structure of solutions is un-

certain and any model of atomistic behaviour in the neighbourhood of a crystal-solution interface is therefore highly speculative. It may be expected that the recent advances in understanding of the liquid state will lead to new experimental and theoretical studies on solutions, and there is considerable scope for original work. The content of this chapter is limited to an explanation of existing theories in order to formulate the most complete model of crystal growth from solution which can be given at present.

4.2. Nucleation

The initial stage of crystallization in a supercooled liquid is the formation of nuclei of the crystalline phase. Crystal growth, as distinct from nucleation, is the process by which these nuclei attain macroscopic dimensions.

The most important early study of nucleation was that of Tammann (1925), who determined the rate of nucleation of complex organic materials. The form of the curve he obtained is shown in Fig. 4.1. On cooling below

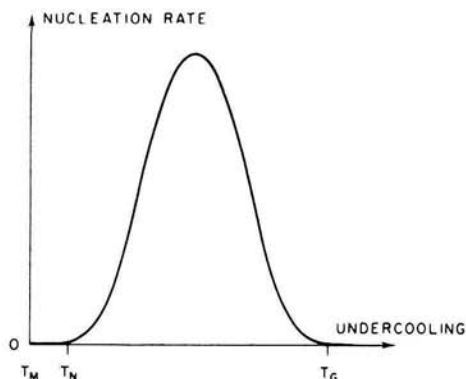


FIG. 4.1. Temperature dependence of nucleation rate (after Tammann, 1925).

the melting point T_M , the nucleation rate is low until some temperature T_N is reached at which the nucleation rate increases very rapidly. The metastable region $T_M \rightarrow T_N$ will depend on such factors as the purity of the melt and the presence of dust or other particles which may act as centres for nucleation. The maximum in the nucleation-temperature curve is due to a slowing down in the kinetics as the temperature is decreased. The fall in the nucleation rate is particularly marked in viscous melts, and will become essentially zero at some temperature T_G . If the melt is cooled to T_G without any crystallization, a glass will be formed. A similar curve to Fig. 4.1 will apply to solutions and it is possible to cool very viscous solutions to a temperature at which nucleation does not occur.

Reviews of nucleation from solution have been given by Hirth and Pound (1963), Nielsen (1964) and Zettlemoyer (1969). In most systems used for the growth of crystals, nucleation occurs heterogeneously, that is at favourable sites within the solution such as the crucible wall or the surface of the solution. Nucleation theory, however, normally describes the process of homogeneous nucleation in which the nuclei are considered to form at random throughout the solution, although estimates of heterogeneous nucleation can also be made.

Fluctuations within the supersaturated solution give rise to small clusters of molecules, known as "embryos". The probability that an embryo will grow to form a stable nucleus depends on the change in free energy associated with its growth or decay. The change in Gibbs free energy associated with the formation of a spherical embryo of radius r is given by

$$\Delta G = 4\pi r^2 \gamma - \frac{4}{3}\pi r^3 \Delta G_V + \Delta G_E + \Delta G_C \quad (4.1)$$

where γ is the interfacial surface energy of the solid phase and ΔG_V the difference in the Gibbs free energy per unit volume between the solid and liquid phases. The terms ΔG_E and ΔG_C represent respectively the changes in Gibbs free energy due to the strain energy and to the configurational entropy change associated with the replacement of internal degrees of freedom of bulk crystal by rotational and translational degrees of freedom of isolated embryos (Lothe and Pound, 1962) and these are normally neglected as a first approximation.

As r increases from zero, the Gibbs free energy increases up to a critical value r^* and then decreases, so that r^* represents the minimum radius of a stable nucleus. The value of r^* is given by differentiation of Eqn (4.1) as

$$r^* = \frac{2\gamma}{\Delta G_V}. \quad (4.2)$$

The form of Eqn (4.2) is unchanged if nuclei of nonspherical shape are considered but the numerical factor will then differ from 2.

The critical radius r^* may be related to the supersaturation in the system if the free-energy change per unit volume is written as

$$\Delta G_V = -S_V \Delta T = \frac{\phi_V}{T} \Delta T \quad (4.3)$$

where ϕ_V is the heat of crystallization per unit volume and ΔT the magnitude of the supercooling at constant pressure. For an ideal solution, the equilibrium solute concentration is given by $n_e = n_\infty \exp(-\phi/RT)$, where ϕ ($=\Delta H_f$) is the molar heat of solution so that $\phi = V_M \phi_V$, with V_M the

molar volume. The relative supersaturation for small values of ΔT is

$$\sigma = \frac{\Delta n}{n_e} = \frac{\phi \Delta T}{RT^2} \quad (4.4)$$

so that

$$\Delta G_V = \frac{\phi_V \Delta T}{T} = \frac{\phi \Delta T}{V_M T} = \frac{RT\sigma}{V_M}. \quad (4.5)$$

Substitution for ΔG_V in Eqn (4.2) gives the value of the critical radius as

$$r^* = \frac{2\gamma V_M}{RT\sigma} \quad (4.6)$$

so that an increase in supersaturation will decrease r^* and will therefore favour nucleation.

The value of ΔG in Eqn (4.1) for a nucleus of critical size is

$$\Delta G^* = \frac{16\pi\gamma^2}{3\Delta G_V^2} = \frac{16\pi\gamma^3 V_M^2}{3R^2 T^2 \sigma^2} \quad (4.7)$$

and, if there are n molecules per unit volume, the concentration of nuclei of critical size is

$$n^* = n \exp(-\Delta G^*/kT). \quad (4.8)$$

The nucleation rate I , being defined as the number of critical nuclei generated in unit volume per second, is given by the product of the concentration of nuclei of critical size and the rate at which molecules join such nuclei as

$$I = n^* z^* A^* = 4\pi n^* z^* r^{*2}. \quad (4.9)$$

Here z^* is the frequency of attachment of single molecules to unit area of nuclei and A^* is the area of a critical nucleus. Substitution for r^* and n^* in Eqn (4.9) gives

$$I = \frac{16\pi z^* \gamma^2 n V_M^2}{R^2 T^2 \sigma^2} \exp\left(-\frac{16\gamma^2 V_M^2}{3kR^2 T^3 \sigma^2}\right) \quad (4.10)$$

from which it is apparent that I will vary rapidly with the supersaturation σ , mainly through the exponential term.

The above treatment follows that given by Volmer and Weber (1926) who assumed that the probability of growth of the nuclei undergoes a sharp discontinuity at the critical radius r^* . Actually embryos of sub-critical size will have a finite probability of growing and those of super-critical size may shrink. A correction for such behaviour was applied by Becker and Döring (1935), but the resulting expression for I still varies

rapidly with the driving force for crystal growth, which is represented by σ .

The dependence on supersaturation of the nucleation rate of potassium sulphate from aqueous solution has been measured by Mullin and Gaska (1969) and is shown in Fig. 4.2. This figure shows a comparison between the nucleation rate and the growth rate over the same supersaturation range. Nucleation is found to be extremely slow for supersaturations below

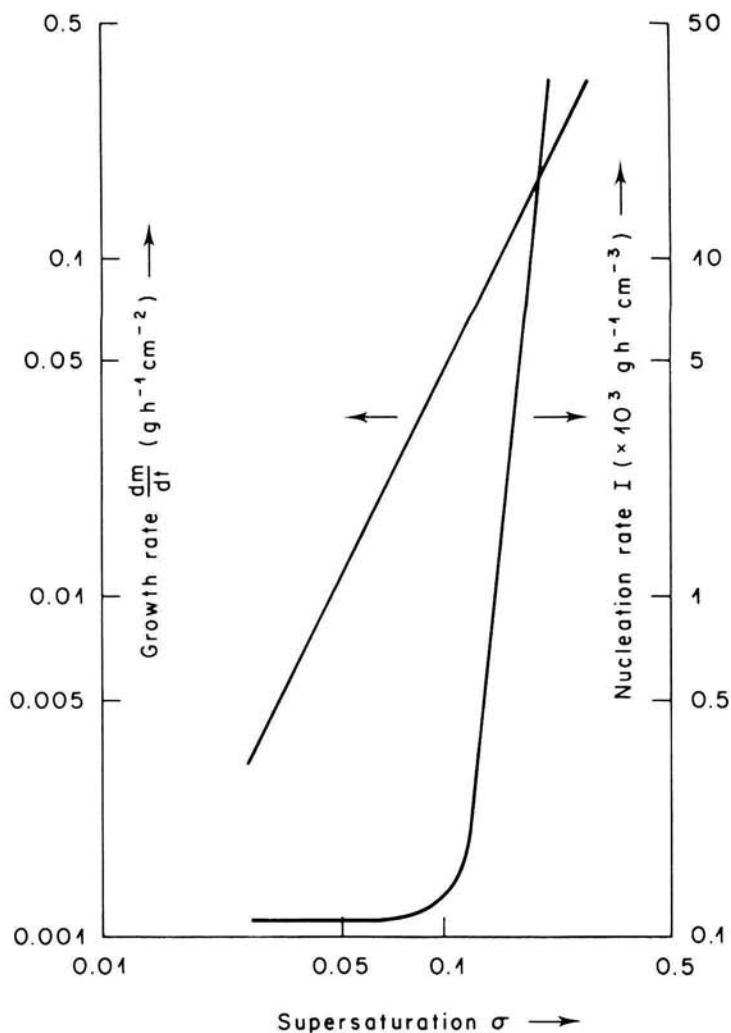


FIG. 4.2. Growth and nucleation rates of potassium sulphate (after Mullin and Gaska, 1969).

10⁰/₀ and so will not interfere to any appreciable extent with growth on established crystals in well-stirred solutions at supersaturations much below this value. The form of the $I(\sigma)$ curve is in quite good agreement with that of Eqn (4.10) and, in the region of supersaturation above 10⁰/₀, the nucleation rate can be approximated by a power law $\sim \sigma^9$.

In the presence of a solid surface or other favourable centre, the nucleation rate increases because of a reduction in the interfacial free energy. An expression for the rate of heterogeneous nucleation may be obtained by replacing ΔG^* by some lower value, depending on the nature of the surface and the shape of the embryos. Foreign particles are well known to provide nucleation centres and the problem of achieving a really clean system makes truly homogeneous nucleation difficult to achieve experimentally.

When the conditions for nucleation are first created in a solution, a finite period is required before the steady nucleation rate is established. The rate at which the nucleation rate approaches the steady value I_0 can be described (Dunning, 1955) by a relation

$$I(t) = I_0 \exp\left(-\frac{\tau}{t}\right).$$

The time constant τ can be written as

$$\tau = \frac{N_C^2 h}{N_S^* kT} \exp\left(\frac{W_D}{kT}\right) \quad (4.11)$$

where N_C is the number of molecules in the critical nucleus and N_S^* the number of solute molecules in the layer of solution adjacent to this nucleus. Cobb and Wallis (1967) have estimated that, in the growth of Al_2O_3 from high-temperature solution, τ can have values from about 0.4 μs to 40 μs for undercoolings between 1°C and 10°C. Under normal growth conditions, therefore, this time dependence should have little effect since undercoolings are expected to be less than 10°C. Long induction periods prior to nucleation may, however, be possible in highly viscous solutions.

4.3. Rough and Smooth Interfaces

Once a crystal has nucleated in a solution, the growth process involves the transport of solute molecules from the solution to some point on the crystal surface where they become part of that surface. Of critical importance is the nature of the crystal-solution interface and we consider first the atomic models of the surfaces of crystals.

To the unaided eye, many crystals grown from solution have perfectly flat faces. The important question which will determine the growth kinetics of the crystal is whether this flatness persists down to the atomic

level. Figure 4.3(a) shows a section through an idealized crystal having atomically flat faces, in which the atoms, all identical, have been represented as small cubes (this picture clearly differs very strongly from reality!). Inside the crystal any atom will have six neighbours and, if the binding energy per atom pair is W_B , the energy with which the atom is bound into the crystal is $3W_B$ since each bond is shared between two atoms. For simplicity, only nearest-neighbour interactions are considered. If a single extra atom is to be added to the crystal, it can form a bond with only one nearest neighbour and so its binding energy is only W_B . Further atoms may, of course, form extra bonds with this first additional atom (adatom) and so constitute a stable cluster, but the small energy with which the first atom is attached is clearly a major barrier to the growth of this crystal.

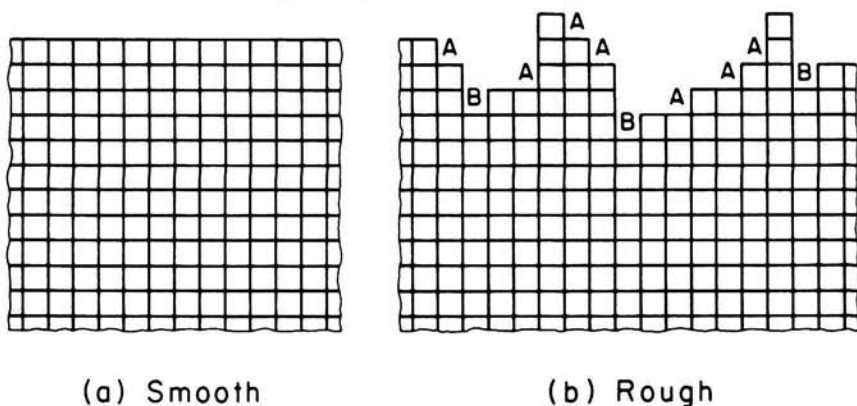


FIG. 4.3. Crystal interfaces. (a) "flat", (b) "rough".

An atomically rough crystal interface will have a cross-section such as that shown diagrammatically in Fig. 4.3(b). An atom added at the sites labelled A will form bonds with two atoms in the same plane and atoms arriving at sites labelled B will form bonds with three atoms in this plane. It is clear that any atom incident on this "rough" surface will have a much greater probability of becoming part of that surface than in the case of the smooth surface. Note that this probability will depend on the binding energy W_B , $2W_B$, $3W_B$, etc., not linearly but through terms $\exp(W_B/kT)$, $\exp(2W_B/kT)$ etc., where T is the interface temperature and k is Boltzmann's constant.

From this very simple argument, we may conclude that atomically rough surfaces have a much higher rate of growth than atomically flat surfaces. Rough surfaces tend to remain rough as long as adatoms which become attached at sites such as those labelled A in Fig. 4.3 create new "corners" for the attachment of subsequent atoms. However, on a smooth surface,

the rate-limiting step will be the addition of a new atom or group of atoms on that surface, since this group will form a layer with a "rough" edge at which atoms can be integrated relatively easily until the layer covers the whole crystal face and the surface is again smooth.

4.4. Models of Surface Roughness

Several calculations have been performed of the degree of roughness of a crystal surface and its variation with temperature. Burton and Cabrera (1949) used the Onsager (1944) solution of the Ising model to treat the behaviour of an array of atoms on the surface of the crystal. If U is the surface potential energy per atom of the actual surface and U_0 that of a perfectly flat surface, the surface roughness is defined as $S_r = (U - U_0)/U_0$. The parameter S_r will clearly be zero for a perfectly flat surface and so a non-zero value of S_r is a measure of the degree of roughness. A simple cubic array (such as that of Fig. 4.3) is treated and is assumed to be perfectly flat at absolute zero.

The energy required to remove an atom from the perfectly flat surface and to place it on a site in the next layer (previously empty) is $2W_B$ since four bonds must be broken. For temperatures well below a critical value T_c , $S_r = 4 \exp(-2W_B/kT)$ in which the factor $\exp(-2W_B/kT)$ is the probability of excitation of a single atom from a full to an empty layer on the surface. The variation of this function with temperature is shown in Fig. 4.4(a). It will be seen that the surface may be assumed flat provided that T is much less than $0.1 W_B/k$. More recent treatments have predicted

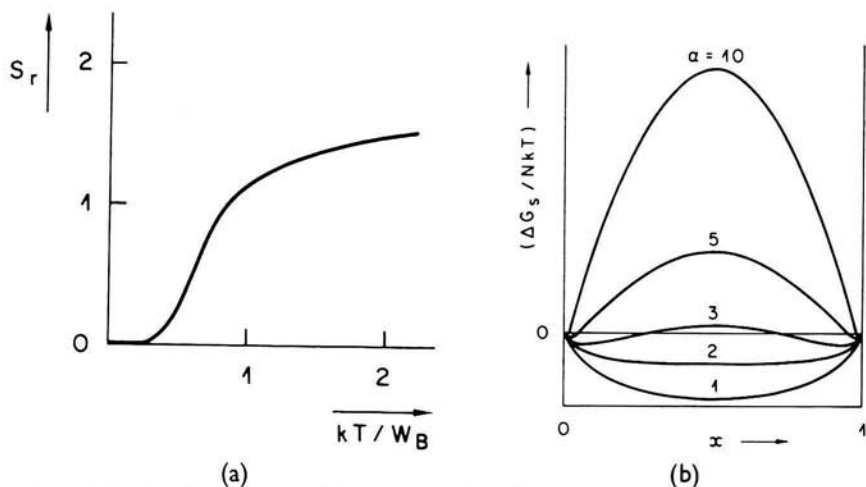


FIG. 4.4. (a) Temperature dependence of surface roughness (after Burton and Cabrera, 1949). (b) Free energy change with fractional occupation of layer (after Jackson, 1958).

curves which differ markedly from that of Fig. 4.4(a), but the trend is always from $S_r=0$ at low temperatures with the roughness increasing rapidly as T is raised above some value in the region of $0.2 W_B/k$. The temperature T_c at which the surface in contact with the vapour becomes "ideally rough" is given by $W_B/k \ln(2^{1/2} - 1)^{-1}$ and is normally much higher than the melting point of the solid. For solid-liquid interfaces W_B is lower and the surface may be rough at or below the melting point.

Jackson (1958) used a rather different approach which takes into account the nature of the medium in contact with the crystal surface. His approximation involves a calculation of the change in the Gibbs free energy as atoms are added to the surface. The results are shown in graphical form in Fig. 4.4(b) as a plot of the change in free energy per atom versus the fraction x of atoms occupying a layer on the surface. The parameter $\alpha = (L/kT)f_k$, where L is the latent heat of the process, and $f_k (<1)$ is a crystallographic factor representing the fraction of all first neighbours lying in a plane parallel to the face considered. It may be seen that, for $\alpha < 2$, the free energy is a minimum when $x = 0.5$, that is when the surface is rough. For $\alpha > 2$, the free energy is a minimum when x has a value close to 0 or 1, that is when the surface is almost smooth. For a {100} plane on a simple cubic lattice, $f_k = 2/3$ and the critical condition $\alpha = 2$ corresponds, for growth from a pure melt, to a melting temperature $T_M = L/3k$.

A similar problem was treated by Temkin (1966), who described the behaviour of the surface in terms of a dimensionless parameter $\gamma' = 4W/kT$, where W is the surface energy per atom. A flat surface corresponds to a high value of γ' . While the Temkin theory is related to that of Jackson, it is more general in that the number of surface layers considered is unlimited.

All the theoretical treatments such as those described suffer from the necessity to make some approximation since a rigorous solution is not possible. The most common approximations are the restriction of interactions to nearest neighbours and the so-called Bragg-Williams approximation which assumes long-range order and averages the interaction between atoms so any effects of small clusters of atoms on each other are not taken into account. Recently attempts have been made to simulate a crystal surface by computer and some results of such simulations have been reported by Binsbergen (1972) and by Bennema and Gilmer (1972). The relatively large size of the simulated surface area ($\sim 40 \times 40$ lattice units) gives more reliable results of the static surface properties like surface roughness than the presently available analytical approaches. Thus computer simulation offers considerable promise.

Hartman and Perdok (1955) proposed a treatment of crystal surfaces based on considerations of the chemical bonding within the crystal. They define periodic bond chains (PBC's) as chains running through the crystal

in certain directions which contain the strongest chemical bonds. The flat (F) crystal faces are those which are parallel to at least two of these chains. Stepped or S faces are those parallel to one PBC and rough or kinked (K) faces are not parallel to any PBC. This theory gives good qualitative results for the crystal morphology of several materials but it cannot be used for quantitative work such as calculations of surface energy.

The observation of smooth, highly reflecting facets on most crystals grown from solutions suggests that these are the F faces. If a small crystal is nucleated with an approximately spherical shape in a supersaturated solution, the rough faces will have more sites available for the attachment of solute molecules and will therefore grow more rapidly. As growth proceeds, these rapidly growing faces tend to disappear and the crystal will eventually be bounded by the relatively slow-growing "habit" faces. The sequence of formation of the habit faces is illustrated in Fig. 4.5. These slow-growing faces, which form the boundaries of crystals grown under stable conditions, are of course not perfectly flat on the atomic scale. They contain vacancies and adatoms (note that the minima in Fig. 4.4(b) for $\alpha > 2$ do not occur exactly at $x=0$ or 1), but their important property is that growth can only occur at certain sites where a new layer is nucleated.

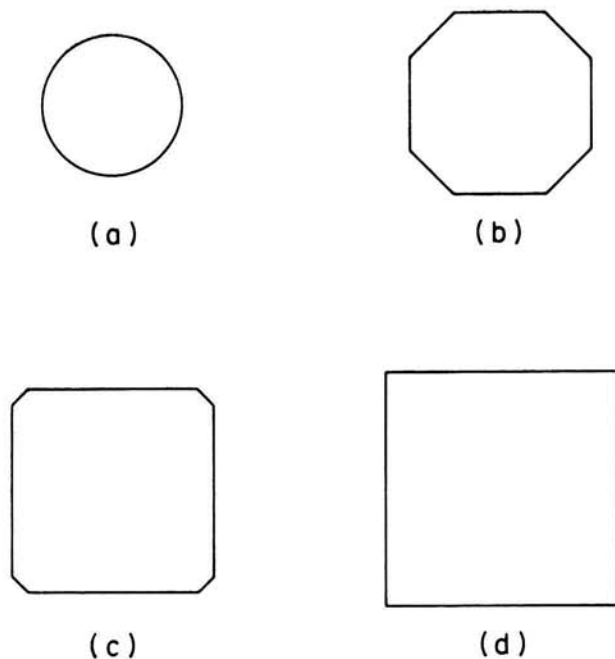


FIG. 4.5. Elimination of more rapidly growing faces during growth.

Such surfaces are referred to as "singular" and correspond to a minimum in the $\gamma(\theta)$ plot which will be discussed in Chapter 5. The mechanisms by which surface nucleation may occur are considered in Section 4.7. It may, however, be noted that the nucleation sites will often be lattice defects, although in principle growth by random two-dimensional nucleation is possible on a singular surface.

Very few observations have been reported of rough surfaces on crystals grown from high-temperature solutions. E. A. D. White (unpublished work) has noted on ruby crystals grown from solution in PbF_2 small facets which appear to be rough, but such facets are very rare and it is probable that they will be observed only when growth is terminated at a transient stage following some change in the experimental conditions which is tending to produce a habit change. Another cause of surface roughness was discussed by Scheel and Elwell (1973b) who assume a fast, unstable growth rate at the end of a crystal-growth experiment due to fast cooling when the furnace is shut off or the crucible is removed so that the remaining solution may be poured out.

The surface roughness of crystals growing in high-temperature solutions will increase with temperature and they may exhibit changes in growth rate or morphology on this account as the growth temperature is raised towards the melting point. However, we shall assume in the subsequent discussion that the faces of crystals grown by this method are atomically flat and the theory will be developed with the assumption that some surface nucleation process is necessary. The experimental evidence for this assumption will be discussed in Sections 4.11 to 4.13.

4.5. Stages in Growth from Solution

As first stressed by Kossel (1927), growth on a crystal having a flat interface requires some mechanism by which atoms (or the appropriate growth units)† will be integrated into the crystal more readily than on the remaining surface. This integration may be at the edge of a layer of monatomic thickness which spreads laterally across the crystal surface. Integration of atoms into the crystal will occur most readily at vacant sites or "kinks" along the edge of this layer since an atom entering such a kink will be able to form nearest-neighbour bonds with three atoms in the crystal. The meaning of the terms "step" and "kink" is illustrated in the diagram of a crystal surface shown in Fig. 4.6.

† Glasner (1973) has proposed that supersaturated aqueous solutions contain crystalline aggregates some 50 to 100 Å in diameter and that crystallization involves the regular arrangement of such aggregates on the crystal surface layers of unit cell height (see Section 4.12) but its confirmation would revolutionize the basic concepts of growth from solutions.

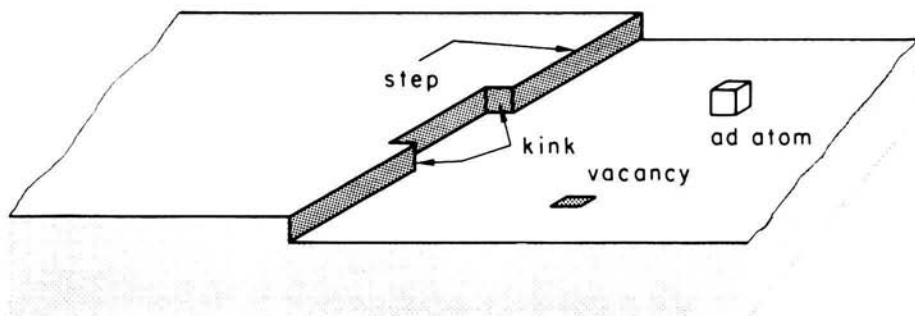


FIG. 4.6. Idealized model of "flat" crystal surface.

If a crystal which has a stepped interface is in contact with a super-saturated solution, the process of growth can be considered to occur in the following stages:

- (i) Transport of solute to the neighbourhood of the crystal surface.
- (ii) Diffusion through a boundary layer, adjacent to the surface, in which a gradient in the solute concentration exists because of depletion of material at the crystal-solution interface.
- (iii) Adsorption on the crystal surface.
- (iv) Diffusion over the surface.
- (v) Attachment to a step.
- (vi) Diffusion along the step.
- (vii) Integration into the crystal at a kink.

The sequence (i)–(vii) is illustrated in Fig. 4.7(a). The detailed nature of the solute particles is not known but it is likely that ions of opposite sign will tend to diffuse together because of their electrostatic attraction. It is certain that some interaction between solute and solvent particles exists in the solution. Such interactions are described by the term *solvation* which is used here to include all forms of interaction. For simplicity the solute particles of Fig. 4.7(a) have been shown to be surrounded in the solution by six particles of the solvent forming a regular octahedron. Solvation may reduce the tendency of solute particles to form clusters near the crystal surface, but the importance of clustering in vapour growth has been demonstrated by Lydtin (1970) and there is a need for experiments aimed at understanding the nature of the solute particles near the crystal interface.

Stages (iii), (v) and (vii) are accompanied by partial desolvation and there will be a new flow of solvent away from the growing crystal. The solute particles may become desorbed at any stage after (iii) and the desorption process has been represented on the diagram by (iv)*. The solute does not

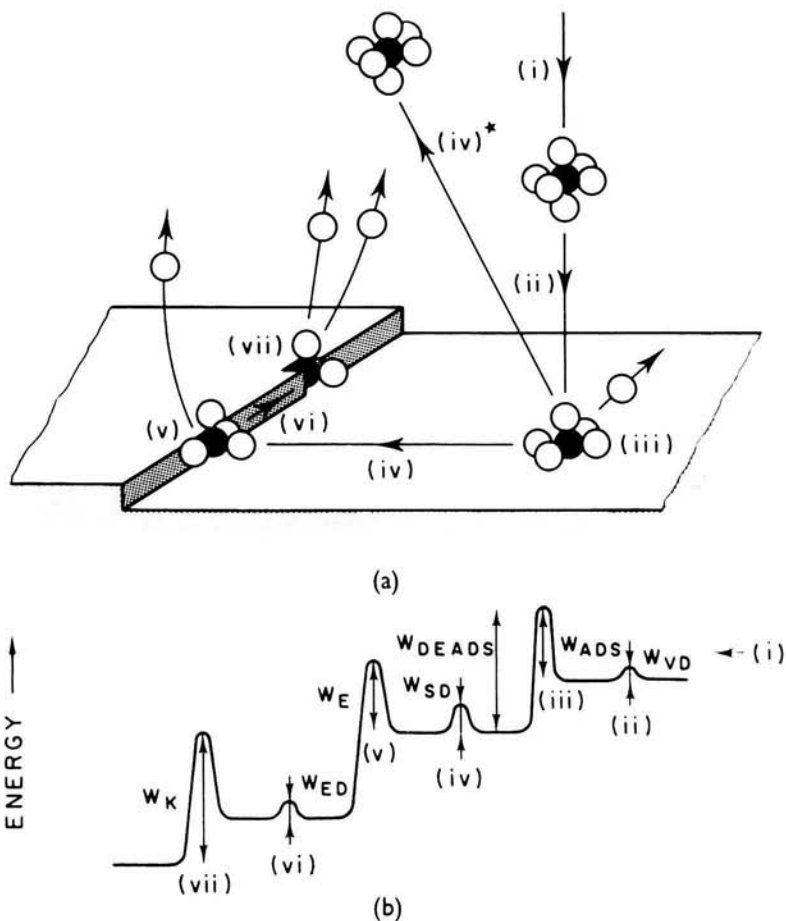


FIG. 4.7. (a) Stages in crystal growth from solution; (b) corresponding energy changes.

fully become part of the crystal until the heat of crystallization has been liberated and the desolvation process is complete.

All the stages in the growth process can be represented by relaxation times or the equivalent energy barriers and the potential energy profile for the growth process is shown schematically in Fig. 4.7(b). A similar diagram was given by Conway and Bockris (1958) for electro-crystallization and by Bennema (1967). An alternative representation would be to consider the various processes as impedances but the electrical analogue of solution growth has not been pursued, presumably because the impedances are distributed rather than discrete.

It should be noted that some of the processes (i)–(vii) occur in series but that some occur in parallel so that not all the stages are necessarily involved in the growth of a chosen material. For example, solute particles may diffuse directly to a kink site by surface migration and so eliminate the necessity for (v) and (vi). Some of the processes will normally occur so quickly (in series) and some so slowly (in parallel) that they may be neglected in comparison with the other stages. In practical crystal growth it is most important to know which process determines the rate of growth and we shall be particularly concerned in this Chapter and in Chapter 6 with the problem of deciding which step is likely to be rate-determining.

In order to discuss the growth process in more detail, it is convenient to take stages (iii)–(vii) together as the interface kinetic stage. It is also necessary to consider the origin of the steps, which has been neglected in the previous discussion. The transport process (stage (i)) by which solute is transferred to the crystal is crucial to the growth of good quality crystals but we defer discussion of this process until Chapter 6, in which the use of the theory in the design of crystal-growth experiments is considered. Stage (ii), diffusion through the boundary layer, is first considered separately for the case in which the interface kinetics are not rate determining. The interface kinetic stage (iii)–(vii) is considered separately and the general case where stages (ii) and (iii)–(iv) are combined is also treated.

4.6. The Boundary Layer

The concept of a boundary or “unstirred” layer was introduced by Noyes and Whitney (1897) and its importance in crystal growth from solution was stressed by Nernst (1904). There is often confusion between the solute diffusion boundary layer, which was introduced in the previous section, and the “hydrodynamic” boundary layer. The latter is a layer of solution which is considered stagnant because of adhesion to the crystal surface while the remainder of the solution is flowing past this surface (see Wilcox, 1969). A simple relation exists between the two layer thicknesses, and the layer referred to in the remainder of the book will be the solute diffusion boundary layer.

A boundary layer, whether diffusion or hydrodynamic, is a simplified concept in any system fluctuating with time. Its use in diffusion-limited growth can be illustrated with reference to a plane crystal surface growing uniformly in a supersaturated solution. The rate of transport of solute per unit area in the z direction, normal to this surface, is given by Fick's law as

$$\frac{dm}{dt} = -D \frac{\partial n}{\partial z} \quad (4.12)$$

and the linear rate of growth of the crystal if its surface at $z=0$ is correspondingly, with n_0 the solute concentration at $z=0$,

$$v = \frac{D}{\rho - n_0} \left(\frac{\partial n}{\partial z} \right)_{z=0} \quad (4.13)$$

where ρ is the density of the crystal.† The solute concentration at the interface will approximate to the equilibrium value provided that the kinetic process is extremely rapid compared with the volume diffusion. This condition was originally assumed by Nernst (1904). If the solute gradient is uniform over the boundary layer, substitution for $(\partial n/\partial z)$ in Eqn (4.13) gives, if $\rho \gg n_0$,

$$v = \frac{D (n_{sn} - n_e)}{\rho \delta} \quad (4.14)$$

This equation may be used to define the width δ of the diffusion boundary layer.

The existence of a boundary layer has been confirmed using optical interference methods by Berg (1938), Bunn (1949) and several other investigators, using aqueous solutions. The solute concentration is determined from the refractive index of the solution and contours of equal concentration around a growing crystal have the form shown in Fig. 4.8.

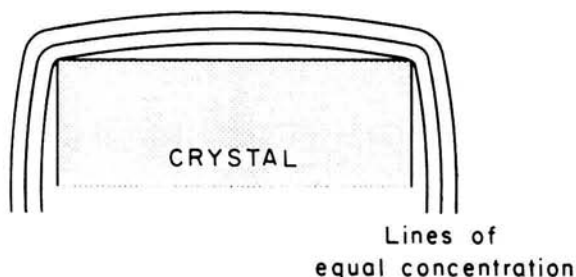


FIG. 4.8. Concentration contours around a growing crystal.

The supersaturation is seen to be highest at the corners and lowest at the centre of the faces. Such a variation of the supersaturation across the face is to be expected for a polyhedral crystal and the experimental results have been explained by Seeger (1953) and by Boscher (1965), who solved the diffusion equation in three dimensions using an electrical analogue.

† The diffusion coefficient D is an effective value, since both positive and negative ions must diffuse and the requirement of local electrical neutrality must be satisfied.

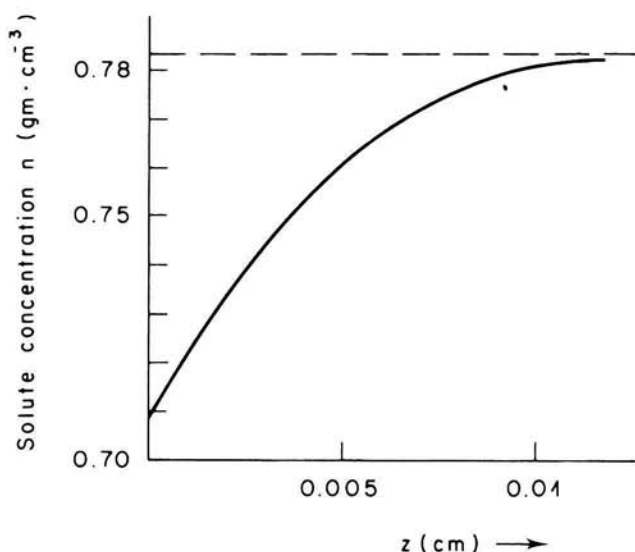


FIG. 4.9. Solute distribution adjacent to growing KBr crystal.

The fact that crystals normally grow uniformly in spite of this variation in supersaturation has been explained by Frank (1958a), who supposed that the rate of growth of any face is determined by the local value of the supersaturation at one point at which the dominant growth centre for the whole face is located. However, if solute is deposited too rapidly from the solution, it may be expected that faster growth will occur at the corners or edges of the crystal where the supersaturation is highest, and this is confirmed by experiment (Chernov, 1963; Lefever and Chase, 1962). The experimental observations of variations in solute concentration across the face of the crystal confirm the approximate nature of equations such as (4.14). The variation of the solute concentration normal to a crystal surface in aqueous solution has been measured by Goldsztaub, Itti and Mussard (1970) and their result is shown in Fig. 4.9. The equation of solute flow in one dimension is normally written in the form

$$D \frac{\partial^2 n}{\partial z^2} + u_{cf} \frac{\partial n}{\partial z} = \frac{\partial n}{\partial t}. \quad (4.15)$$

The first term represents the diffusional flow, the second growth-induced convection (Wilcox, 1972) and the third takes into account the time dependence of the solute concentration. In the steady state, $\partial n / \partial t = 0$ and so, if u is negligible,

$$\frac{\partial^2 n}{\partial z^2} = 0 \quad \text{i.e.} \quad \frac{\partial n}{\partial z} = \text{const} = \frac{n_{sn} - n_c}{\delta}$$

as in Eqn (4.14). The non-linearity in Fig. 4.9 is attributed to convection in the cell used by Goldsztaub *et al.* If the convection term is negligible, the time-dependent solution of Eqn (4.15) has the form

$$n(z, t) = n_e + (n_{sn} - n_e) \operatorname{erf} \left(\frac{z}{2(Dt)^{1/2}} \right). \quad (4.16)$$

The value of the boundary-layer thickness in this case will be time-dependent and integration of the growth rate over the period of the experiment is necessary if a comparison between experiment and theory is to be made.

The problem of the boundary layer was considered by Carlson (1958) who assumed laminar flow of the solution over a face of the crystal. He found that, for uniform growth of the crystal face, the concentration of solute should decrease with distance from the leading edge. As in diffusional flow, therefore, a non-uniform supersaturation over the surface is expected. Carlson derived an expression for the rate of growth of the crystal and his results give for the solute diffusion boundary-layer thickness (taking into account hydrodynamics)

$$\delta = \left\{ 0.463 \left(\frac{\eta}{\rho_{sn} D} \right)^{1/3} \left(\frac{u \rho_{sn}}{\eta l} \right)^{1/2} \right\}^{-1}. \quad (4.17)$$

Here η is the viscosity and ρ_{sn} the density of the solution, u the flow velocity and l the length of the crystal face considered. A similar expression was used by Bennema (1967) to calculate the boundary-layer thickness and the results were found to be in agreement with his experimental values. If $\eta = 10$ cP, $\rho_{sn} = 5$ g cm⁻³, $D = 10^{-5}$ cm² s⁻¹, $u = 0.1$ cm s⁻¹ and $l = 5$ mm, the value of δ is calculated to be 0.055 cm and this value is probably correct to the order of magnitude for diffusion-controlled growth.

The variation of δ with the solution flow rate u may be used to explain the change in crystal-growth rate at high supersaturation when the flow rate is varied. The usual form of the variation of the crystal-growth rate in aqueous solutions with the solution flow rate is shown in Fig. 4.10. The increase in growth rate with flow rate continues until some limiting rate is reached where the growth rate becomes controlled by the interface kinetic process. Carlson's theory predicts that δ should vary as $u^{-1/2}$, and so v should depend on $u^{1/2}$. This result is in reasonable agreement with the experiments of Hixson and Knox (1951), who report $v \propto u^{0.60}$, and of Mullin and Garside (1967), whose results are described by a relation $v \propto u^{0.65}$.

A similar variation in the growth rate is observed when a crystal is

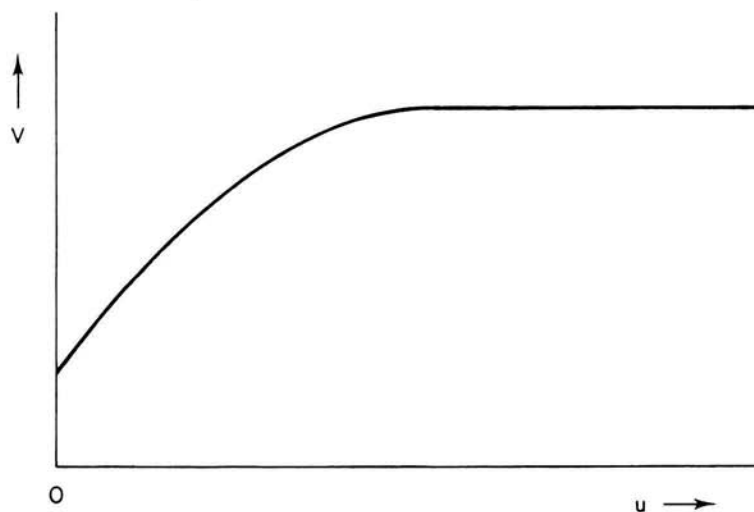


FIG. 4.10. Variation in linear growth rate with solution flow rate.

rotated in solution. The boundary-layer thickness in this case is given by Burton, Prim and Slichter (1953) as

$$\delta \simeq 2^{2/3} D^{1/3} \nu^{1/6} \omega^{-1/2} \quad (4.18)$$

where ω is the angular velocity of rotation of the crystal and ν the kinematic viscosity of the solution. A linear dependence of the growth rate v on $\omega^{1/2}$ is found for the growth of sodium thiosulphate using the data of Coulson and Richardson (1956), for low values of ω . Laudise, Linares and Dearborn (1962) measured the variation of the growth rate of yttrium iron garnet from solution in $\text{BaO}-\text{B}_2\text{O}_3$ with crystal rotation rate. They found an increase in v for values of ω up to about 50 r.p.m., beyond which the growth rate was independent of the rotation rate. The data are insufficient to confirm an $\omega^{1/2}$ dependence at low rotation rates.

In general the observed rate of growth of a crystal will depend partly on boundary-layer diffusion and partly on the interface kinetics. Brice (1967a) has shown how the role of the boundary layer may be taken into account in order to deduce the form of the interface kinetic law. His approach is based on that of Berthoud (1912) and Valetton (1924). The solute concentration at the interface is taken as n_i and the kinetic law is assumed to have the form

$$v = A(n_i - n_c)^m \quad (4.19)$$

where A and m are independent of the solute concentration. The growth law may also be expressed in terms of the diffusional flow by a modification of Eqn (4.14). In this case

$$v = \frac{D(n_{sn} - n_i)}{\rho \delta} \quad (4.20)$$

Elimination of n_i between Eqns (4.19) and (4.20) gives

$$\left(\frac{v}{A}\right)^{1/m} + \left(\frac{v\rho\delta}{D}\right) = n_{sn} - n_e \quad (4.21)$$

If δ varies as $\omega^{-1/2}$ or as $u^{-1/2}$, a plot of $v^{1/m}$ versus $v\omega^{-1/2}$ or $vu^{-1/2}$ at constant supersaturation should be linear and such plots were successfully used by Brice to obtain the power m of the kinetic law. This procedure does not, however, give satisfactory results in all cases, presumably because of the simplifications introduced in assuming Eqns (4.19) and (4.20).

The variation of growth rate with boundary-layer thickness as a function of supersaturation was discussed by Scheel and Elwell (1973a) and will be treated in Chapter 6. For low and medium supersaturation Eqn (4.21) will approximately hold. However, at high supersaturation and sufficient stirring a maximum (stable) growth rate is reached which is a constant for a given solute-solvent system. Depending on n_{sn} this maximum growth rate is determined either by surface kinetics or by heat flow.

4.7. Generation of Surface Steps

We now consider interface kinetic mechanisms in detail, treating in particular crystal surfaces which are "flat" rather than "rough". The critical step in the growth of crystals having perfect or nearly perfect surfaces is the formation of a cluster of atoms sufficiently large to constitute a stable nucleus which will grow to form a new layer. The classical theory of crystal growth is analogous to the nucleation theory described in Section 4.2, with the exception that nucleation occurs on a crystal surface. In such a "two-dimensional" nucleation theory it is convenient to treat a cylindrical embryo of radius r and of height a corresponding to one growth unit (e.g. an atom or molecule). The change in Gibbs free energy on formation of such an embryo is

$$\Delta G(r) = 2\pi r\gamma_e - \pi r^2 a \Delta G_v \quad (4.22a)$$

where γ_e is the edge energy per unit length of the nucleus. The term ΔG_e of Eqn (4.1) is included (see Lewis, 1974) by putting

$$n(r) = n_0 \exp(-\Delta G/kT) \quad (4.22b)$$

where n_0 is the density of available sites.

Alternatively the free energy can be expressed in terms of the energy per growth unit (for simplicity, we shall use the term "molecule") γ_m on the edge of the cylindrical nucleus. If the length of the molecule is also a , $\gamma_m \simeq a\gamma_e$ and so

$$\Delta G \simeq \frac{2\pi r \gamma_m}{a} - \pi r^2 a \Delta G_v, \quad (4.23)$$

and differentiation gives the radius of the critical nucleus as

$$r_s = \frac{\gamma_m}{a^2 \Delta G_v} \quad (4.24a)$$

and the corresponding value of ΔG is

$$\Delta G^* = \frac{\pi \gamma_m^2}{a^3 \Delta G_v}. \quad (4.24b)$$

Substitution for ΔG_v from Eqn (4.5) gives

$$r_s^* = \frac{\gamma_m V_M}{a^2 R T \sigma}.$$

A more familiar form of this equation is obtained by putting $V_M = N_A a^3$, where N_A is Avogadro's number and the molecule is assumed to be a cube of side a . This gives

$$r_s^* = \frac{\gamma_m a}{k T \sigma} \quad (4.25a)$$

and correspondingly

$$\Delta G^* = \pi \gamma_m^2 / k T \sigma. \quad (4.25b)$$

The number i^* of molecules in a critical nucleus is

$$i^* = \frac{\pi r_s^{*2}}{a^2} = \left(\frac{\gamma_m}{k T \sigma} \right)^2. \quad (4.25c)$$

The rate of surface nucleation, and hence of crystal growth, depends by analogy with Eqn (4.8) on $\exp(-\Delta G^*/kT)$, and it is instructive to estimate the order of magnitude of this factor as a function of the supersaturation. The energy γ_m is of the order of the binding energy W_B , introduced in Section 4.3, that is $\gamma_m \simeq \phi_m/6$, where W_B is the binding energy, ϕ_m is the heat of solution per molecule. (Strictly, the value of γ_m will be higher on low energy planes.) Using a value for $\phi = 72$ kJ mole⁻¹ as found for nickel ferrite in barium borate (Elwell, Neate and Smith, 1969) so that $\phi_m \sim 2 \times 10^{-20}$ J molecule⁻¹, then, with $T = 1500$ K, $\gamma_m/kT \simeq 1$ so that $\Delta G^* \simeq \pi/\sigma$. The term $\exp(-G^*/kT)$ varies from 3×10^{-3} for $\sigma = 0.5$ and $\sim 10^{-13}$ for $\sigma = 0.1$ to $\sim 10^{-130}$ for $\sigma = 0.01$. Growth by two-dimensional nucleation therefore has a high probability except at very low supersaturation values. In the system referred to above, growth was observed experimentally at relative supersaturations down to about 1%.

A discrepancy between observed growth rates from the vapour at supersaturations below 1% and the prediction from two-dimensional nucleation theory of negligible growth below 50% supersaturation (for $\phi_m/kT \simeq 12$) led Frank (1949) to propose that dislocations having a screw component act as a continuous source of layers on the surface of a crystal. The presence of the step associated with such a dislocation removes the need for surface nucleation.

Figure 4.11(a) shows the face of a crystal with a screw dislocation emerging at P . Molecules are readily integrated into the crystal at the step PQ , which is of approximately monomolecular height, and the initial growth is normal to the step as indicated by the arrow. The emergence of the screw dislocation at P fixes this point so that the rate of movement of

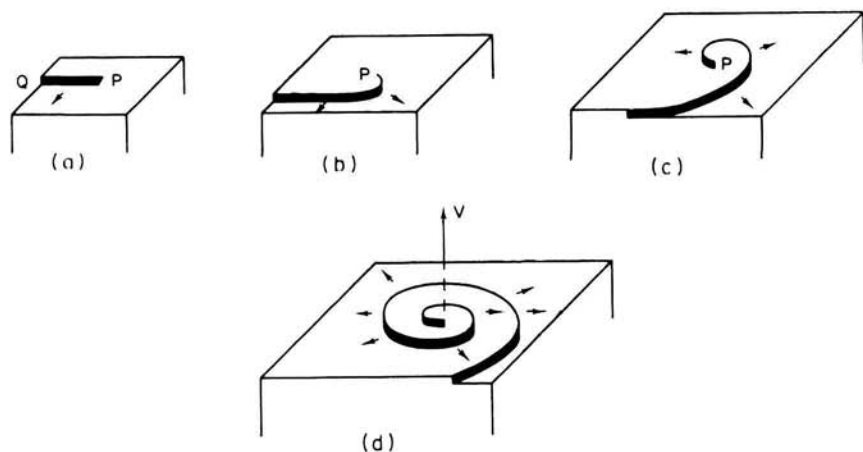


FIG. 4.11. Development of a spiral.

the layer is here zero. Elsewhere the step moves in such a way that its linear velocity is constant and angular velocity decreases with the distance from P . As the crystal grows, the step therefore winds itself up into a spiral with its centre at P . The development of the spiral is illustrated in Figs 4.11(a)–(d). In this sequence the face considered grows normal to itself at a linear rate v . The area of the face increases at the same time, due to a similar growth process on the other surfaces of the crystal. The spiral will continue to wind itself up until the separation of adjacent layers at the centre is of the order of the radius r_s^* of the critical nucleus.

The presence of growth spirals has now been established on a large variety of crystals. These include natural crystals (Sunagawa, 1960) and synthetic crystals grown from the vapour phase (Verma, 1953) and from



FIG. 4.12. Growth spiral on a rare-earth orthoferrite crystal (after Tolksdorf and Welz, 1972).

aqueous solution (Forty, 1951). Figure 4.12 shows a particularly beautiful example of a growth spiral on an orthoferrite crystal grown from high-temperature solution, observed by Tolksdorf and Welz (1972). The presence of such spirals provides evidence for the validity of Frank's screw-dislocation model, although the height of the steps in Fig. 4.12 is 50–150 Å rather than of monomolecular dimensions as envisaged by Frank.

Lewis (1974), in a review of two-dimensional nucleation, has pointed out that the importance of growth in solution by this mechanism has been underestimated, certainly for medium and high supersaturation. As is clear from Eqn (4.25), the probability of 2-D nucleation will depend on the factor ϕ_m/kT , which will be lower for solution growth than for growth from the vapour. Bennema *et al.* (1972) have confirmed by computer simulation experiments that a mechanism of growth by 2-D nucleation on growing two-dimensional nuclei can describe some experimental growth-rate data better than the screw-dislocation theory.

4.8. The Theory of Burton, Cabrera and Frank

Screw dislocations are important because they can provide a continuous source of steps which can propagate across the surface of the crystal. In order to construct a theory which will predict values for the rate of growth of the crystal, it is necessary to calculate the rate at which molecules will arrive at the steps of the spiral. A theory of crystal growth including the mechanism of step generation and of transport into the step was given by Burton, Cabrera and Frank (1951) and this BCF paper has assumed great importance since much of the content will apply to any theory of crystal growth. The theory given here was originally proposed for growth from the vapour phase but its applicability to solution growth has been strongly advocated by Bennema (1965, 1967) and by Bennema and Gilmer (1973) whose treatment we follow.

The velocity of growth will depend on the shape of the growth spiral, for which an exact expression has not been developed. BCF used the equation for an Archimedian spiral

$$r = 2r_s^* \theta \quad (4.26)$$

where r and θ are the coordinates of any point on the spiral as indicated in Fig. 4.13. Equation (4.26) should be a good approximation to the behaviour of a real spiral, for positions not too close to the centre. The distance y_o between the steps of the spiral will thus be

$$y_o = 2r_s^*(\theta + 2\pi) - \theta = 4\pi r_s^*$$

A more rigorous approach by Cabrera and Levine (1956) showed that a better approximation is given by

$$y_0 \simeq 19r_s^* = \frac{19\gamma_m a}{kT\sigma} \quad (4.27)$$

and this value will be used in the subsequent development.

The second part of the BCF theory is concerned with the transport of molecules from the bulk of the solution to kinks in the steps of the spiral. It is assumed that the surface-diffusion coefficient is independent of the local concentration and this, together with the neglect of surface vacancies, is the main assumption of the theory. As mentioned earlier, the nature of

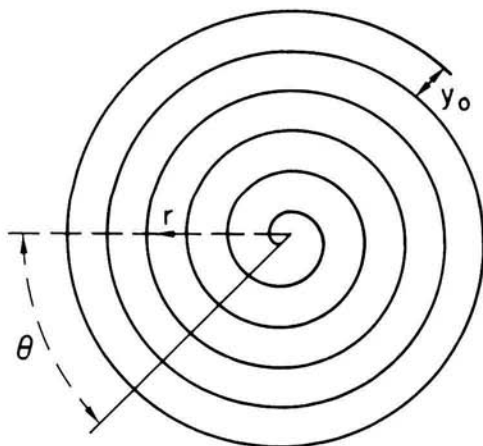


FIG. 4.13. Growth spiral.

solute particles on the crystal surface is not known but, if local electrical neutrality is assumed, it is possible to define a single relaxation time for each stage of the surface transport process in the same way that an effective volume-diffusion coefficient can be specified for the flow of ions of opposite charge.

The steps in the spiral are assumed to move negligibly slowly compared with the rate of migration of molecules on the surface. This assumption is justified since the rate at which the step moves is governed by the rate of arrival of diffusing molecules. For simplicity, the distance from the spiral centre is taken to be so large that curvature of the steps may be neglected. The net flux of particles into a strip of width dy on the surface in the region of a step will depend upon the flux j_v from the solution to the surface and on the flux j_s across the surface into the step due to the concentration gradient created by integration of molecules into the surface at the step.

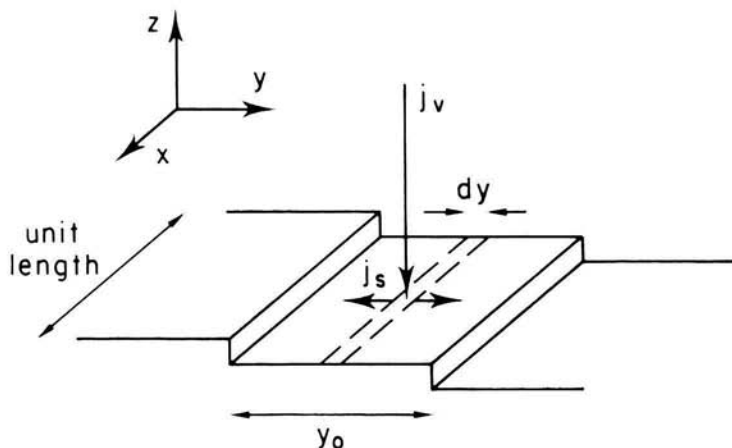


FIG. 4.14. Flow of solute to a step.

These particle fluxes are indicated in Fig. 4.14. In the steady state the two fluxes will balance and so, for unit length in the x direction,

$$\frac{dj_s(y)}{dy} - j_v = 0. \quad (4.28)$$

The surface flux j_s can be expressed in terms of the surface-diffusion coefficient D_s and the local surface concentration n_s as

$$j_s = -D_s \frac{dn_s}{dy} = -D_s \frac{d}{dy} (n_{se} \sigma_s + n_{se}) = -D_s n_{se} \frac{d\sigma_s}{dy} \quad (4.29)$$

where n_{se} is the equilibrium concentration at the surface far from a step and σ_s the local value of the relative supersaturation. It is convenient to introduce a variable ψ as the difference between the surface supersaturation σ_s and the supersaturation very far from a step, which is governed by the solute concentration in the bulk of the solution. Thus

$$\psi = \sigma - \sigma_s(y) \quad (4.30)$$

and, since σ is independent of y ,

$$j_s = D_s n_{se} \frac{d}{dy} (\sigma - \sigma_s) = D_s n_{se} \frac{d\psi}{dy}. \quad (4.31)$$

The flux j_v can be written as the difference between the flux leaving the surface $n_s(y)/\tau_{\text{deads}}$ and that moving towards the surface $n_{se}/\tau_{\text{deads}}$ where τ_{deads} is the relaxation time governing desorption of solute from the surface (shown as (iv)* in Fig. 4.7). Thus

$$j_s = \frac{\sigma n_{sr} - n_s}{\tau_{\text{deads}}} = \frac{n_{sr}(\sigma - \sigma_s)}{\tau_{\text{deads}}} = \frac{n_{sr} \psi}{\tau_{\text{deads}}}. \quad (4.32)$$

On substitution of Eqns (4.31) and (4.32) into Eqn (4.28), the differential equation of solute transport becomes

$$D_s \tau_{\text{deads}} \frac{d^2 \psi}{dy^2} = \psi$$

or

$$y_s^2 \frac{d^2 \psi}{dy^2} - \psi = 0 \quad (4.33)$$

where $y_s = \sqrt{(D_s \tau_{\text{deads}})}$ is the mean distance travelled by solute molecules on the surface. Equation (4.33) has a general solution

$$\psi = A \exp(y/y_s) + B \exp(-y/y_s) \quad (4.34)$$

and it is necessary to introduce boundary conditions to obtain values for A and B . The most probable situation is that $y_s \gg x_n$, where x_n is the average distance between kinks in a step. For a set of equidistant steps of separation y_n and with the origin of y chosen to be mid-way between the steps, the boundary condition may be expressed by putting the value of ψ at a step as $\beta\sigma$, so that $\psi = \beta\sigma$ when $y = \pm \frac{1}{2}y_n$. Then, from Eqn (4.34), for $y = +\frac{1}{2}y_n$, $\psi = \beta\sigma = A \exp(y_n/2y_s) + B \exp(-y_n/2y_s)$ and for $y = -\frac{1}{2}y_n$, $\psi = \beta\sigma = A \exp(-y_n/2y_s) + B \exp(y_n/2y_s)$ from which $A = B$, and substitution in terms of $\beta\sigma$ in Eqn (4.34) gives

$$\psi = \frac{\beta\sigma \cosh(y/y_s)}{\cosh(y_n/2y_s)}. \quad (4.35)$$

If $x_n \gg y_s$, it is necessary to introduce an extra factor c_n into Eqn (4.35) to take into account the non-planar diffusion fields around the kinks.

From Eqn (4.31), the flux of particles towards a step may now be written as

$$j_s = D_s n_{sr} \frac{d\psi}{dy} = \frac{D_s n_{sr} \beta\sigma}{y_s} \frac{\sinh(y/y_s)}{\cosh(y_n/2y_s)}. \quad (4.36)$$

If n_{sr} is measured in g cm^{-2} , j_s represents the flux in $\text{g cm}^{-1} \text{s}^{-1}$ towards a step either of monomolecular or larger height. The linear rate of advance of the step v_{st} is obtained by multiplying j_s by the area $1/\rho a$ per unit mass of the crystal so that, for a step of monatomic height,

$$v_{st} = 2j_{s(y=y_n/2)} \cdot \frac{1}{\rho a} = \frac{2D_s n_{sr} \beta\sigma}{\rho a y_s} \tanh \frac{y_n}{2y_s}. \quad (4.37)$$

The factor 2 is introduced since molecules enter the step from two sides.

In order to calculate the linear growth rate v of the crystal (in the z direction), it is necessary to multiply the flux of steps by the height of a step. For a step separation y_o , the number of steps per unit length is $1/y_o$ and so the flux of steps in the y direction will be v_{st}/y_o . If the step height is a , the rate of growth will then be

$$\boxed{v = \frac{v_{st} a}{y_o}} \quad (4.38)$$

or, on substituting for v_{st} and y_o from Eqns (4.37) and (4.27)

$$v = \frac{2D_s n_{se} \beta \sigma^2 k T}{19\gamma_m y_s \rho a} \tanh \frac{y_o}{2y_s} \quad (4.39)$$

If a parameter σ_1 is defined as

$$\boxed{\sigma_1 = \frac{\sigma y_o}{2y_s} = \frac{9.5\gamma_m a}{k T y_s}} \quad (4.40)$$

Eqn (4.39) may be rewritten in the form

$$\boxed{v = \frac{D_s n_{se} \beta}{y_s^2 \rho} \cdot \frac{\sigma^2}{\sigma_1} \tanh \frac{\sigma_1}{\sigma} = \frac{C\sigma^2}{\sigma_1} \tanh \frac{\sigma_1}{\sigma}} \quad (4.41)$$

The variation of growth rate with supersaturation thus depends on two parameters: $C (= D_s n_{se} \beta / y_s^2 \rho)$, which determines the absolute value of v , and σ_1 which determines the shape of the $v(\sigma)$ curve. For low values of $\sigma (\sigma \ll \sigma_1)$ Eqn (4.41) may be approximated by

$$v \simeq \frac{C\sigma^2 (\exp (2\sigma_1/\sigma) - 1)}{\sigma_1 (\exp (2\sigma_1/\sigma) + 1)} \simeq \frac{C\sigma^2}{\sigma_1} \quad (4.42a)$$

while for $\sigma \gg \sigma_1$

$$v \simeq \frac{C\sigma^2 (1 + (2\sigma_1/\sigma) + \dots) - 1}{\sigma_1 (1 + (2\sigma_1/\sigma) + \dots) + 1} \simeq C\sigma \quad (4.42b)$$

The BCF theory therefore predicts a quadratic $v(\sigma)$ curve for low values of the supersaturation with a gradual transition to a linear law as the supersaturation is increased above a critical value σ_1 . A relatively large value of σ_1 for a given material should result in a quadratic growth curve while a linear $v(\sigma)$ plot should be expected according to the above theory if σ_1 is low.

Cabrera and Coleman (1963) have pointed out that at higher supersaturations, the surface supersaturation near the centre of the spiral may be lower than σ because of the depletion caused by surface diffusion to that portion of the spiral where the step spacing y_o is small. The result is that y_o decreases more slowly with σ than predicted by Eqn (4.27). This "back stress" effect makes the transition from a quadratic to a linear law occur at higher values of σ than predicted by Eqn (4.42) and a perfectly linear law is unlikely over any wide range of supersaturation values.

If a number of screw dislocations emerge at the growth centre the form of the spiral will be more complex than that shown in Fig. 4.13. In order to take into account the effect of cooperation between a number of interacting spirals, BCF introduced a factor ϵ such that

$$y_o = \frac{19r_s^*}{\epsilon} = \frac{19\gamma_m a}{\epsilon kT\sigma}. \quad (4.43)$$

Equation (4.41) then becomes

$$v = \frac{C\epsilon\sigma^2}{\sigma_1} \tanh \frac{\sigma_1}{\epsilon\sigma}. \quad (4.44)$$

The factor ϵ can be quite complex and some examples of cooperating dislocations will be discussed in Section 4.12.

BCF Theory of Solution Growth

As mentioned earlier, the BCF theory was derived for growth from the vapour. In the case of solution growth, the molecules were assumed to enter the kinks directly rather than by entering an adsorption layer and undergoing surface diffusion. The justification for this assumption was that the coefficient of volume diffusion ($\sim 10^{-5} \text{ cm}^2 \text{ s}^{-1}$) is normally much higher than the coefficient of surface diffusion ($\sim 10^{-8} \text{ cm}^2 \text{ s}^{-1}$) for molecules in solution so that any diffusion in a direction parallel to the crystal surface might be expected to occur in the boundary layer. If the rate of flow of solute molecules to the kinks is governed by diffusion through the boundary layer, the net flux reaching the steps, which governs their rate of advance v_{st} , will be proportional to the supersaturation σ . With $1/y_o \propto \sigma$ according to Eqn (4.27), the growth rate v will again vary as σ^2 since $v = v_{st} a/y_o$ [Eqn (4.38)]. BCF considered solute flow towards a kink in a hemispherical diffusion field and obtained an expression for the step velocity

$$v_{st} = \frac{Dn_s}{\rho x_o} \left[1 + \frac{2\pi a(\delta - y_o)}{x_o y_o} + \frac{2a}{x_o} \ln \left(\frac{y_o}{x_o} \right) \right]^{-1}. \quad (4.45)$$

For low supersaturations y_o is large and the third term in the bracket is the

dominant one. In this case, $v_{st} \propto \sigma$ and a quadratic law is predicted using Eqn (4.38) since $y_o \propto 1/\sigma$. However, at high supersaturations the second term is dominant since y_o becomes small. In the latter case

$$v_{st} \simeq \frac{Dn_c \sigma y_o}{\rho a(\delta - y_o)}$$

and, neglecting y_o in comparison with δ , Eqn (4.38) gives the growth rate as

$$v = \frac{Dn_c \sigma}{\rho \delta}.$$

This case is exactly the same volume-diffusion limited situation which was considered by Nernst and described by Eqn (4.14).

4.9. Should Surface Diffusion be Included?

The difference between Bennema's treatment of solution growth and the BCF solution-growth theory rests upon whether or not surface diffusion plays an important role in the growth process. It is generally accepted that the rate of volume diffusion exceeds that of surface diffusion, but the effective area of the kink sites is small compared with the total area of the crystal face and this factor will favour a mechanism in which volume diffusion to a random point on the surface is followed by surface diffusion to a kink.

A meaningful numerical comparison between the growth rates calculated using Eqns (4.44) and (4.45) is difficult because many of the parameters in these equations are not known even to the order of magnitude. An attempted comparison is given in Fig. 4.15. In this example it has been assumed that $D = 10^{-5} \text{ cm}^2 \text{ s}^{-1}$, $n_c = 1 \text{ g cm}^{-3}$, $\rho = 5 \text{ g cm}^{-3}$, $a = 4 \times 10^{-8} \text{ cm}$ and $\gamma_m = 2 \times 10^{-20} \text{ J/molecule} \simeq kT$ so that, from Eqn (4.27), $y_o \simeq 10a/\sigma$. The mean separation between kinks x_o is given by BCF as

$$x_o = \frac{a}{2} \exp(W_B/kT) \quad (4.46)$$

and, with the binding energy $W_B \sim \gamma_m \sim kT$ for $T = 1500 \text{ K}$, $x_o \sim a$. BCF estimate $x_o \sim 4a$ and so, for our example, we take an intermediate value of $x_o = 2a$. The boundary-layer width δ is taken to be 10^{-2} cm and the supersaturation range chosen is typical of experimental values. It is found that, with these data, the second term of Eqn (4.45) is dominant and so the growth rate in the BCF solution-growth theory is determined by volume diffusion over the whole range considered. For the surface-diffusion case we assume $D_s = 10^{-8} \text{ cm}^2 \text{ s}^{-1}$ and $y_s = 10^{-5} \text{ cm}$, which are typical values for aqueous solution growth according to Bennema's interpretation

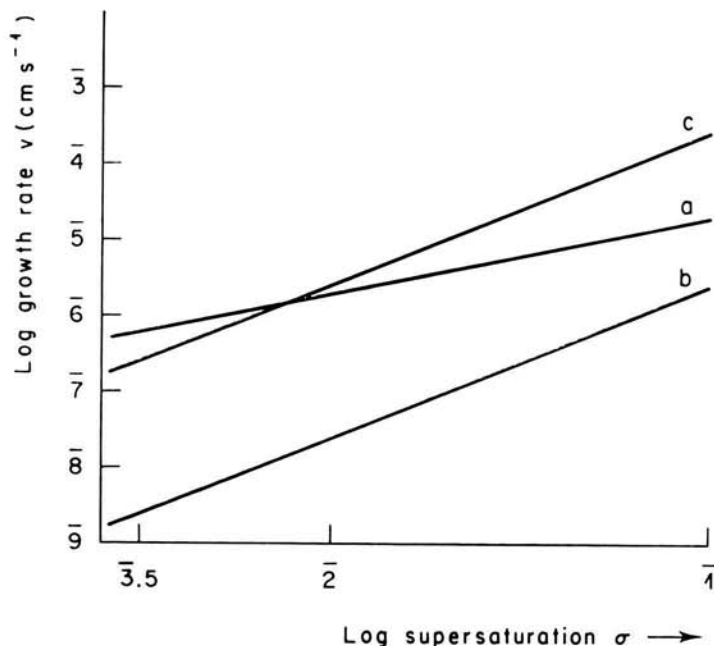


FIG. 4.15. Growth rate for BCF volume and surface-diffusion theories: (a) volume diffusion, (b) surface diffusion, $\beta = 10^{-2}$, (c) surface diffusion, $\beta = 1$.

(Bennema, 1965). The latter value gives $\sigma_1 \simeq .04$ which is within the range of supersaturation values considered. The value of the growth rate for the surface-diffusion model depends critically on the parameter β of Eqn (4.35). A value $\beta \simeq 1$ would indicate that the surface supersaturation has its maximum value and so corresponds to a maximum growth rate. Bennema's estimates of the relevant activation energies suggest a value of $\beta \sim 10^{-2}$ and the usual values are probably somewhere between these limits. There is no reason in principle why a factor β should not be included in Eqn (4.45) also. Figure 4.15 shows that v varies as σ^2 in the supersaturation range shown.

It should be emphasized that the data of Fig. 4.15 represent typical values and do not indicate the effect of surface diffusion on the system considered. Surface diffusion will always increase the growth rate, if its effect is not negligible, by increasing the probability that a solute molecule will find a kink site. Chernov (1961) also proposed a theory of crystal growth from solution based on calculation of the flow to a system of parallel steps, assuming no surface or edge diffusion. The concentration n is assumed to be described by an equation

$$D \frac{\partial n}{\partial r} = A(n - n_c)$$

where n is the concentration at a distance r from a step and A a constant which is large if the kink separation is small. Figure 4.16 shows the solute diffusion field around the steps assumed by Chernov. The solution of the diffusion equation gives for the growth rate

$$v = \frac{AakTn_c}{4\gamma} \frac{\sigma^2}{\{1 + (Aa/D) \ln(\delta\sigma_3/a\sigma) \sinh(\sigma/\sigma_3)\}} \quad (4.47)$$

where $\sigma_3 = 4V_m\gamma/kT\delta$. Eqn (4.47) gives a rather similar result for the growth rate to that of the BCF volume-diffusion theory; at low supersaturations

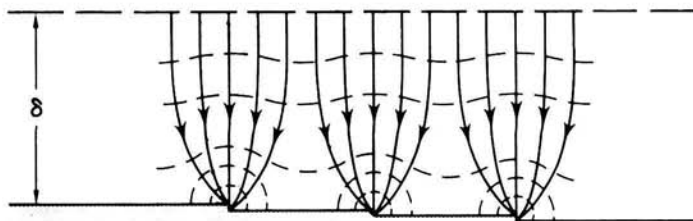


FIG. 4.16. Solute diffusion to system of steps (after Chernov, 1961, 1963).

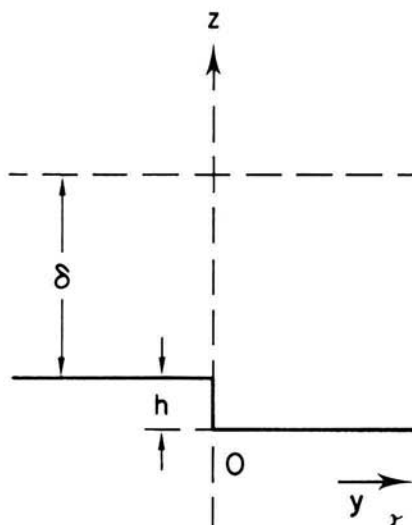
($\sigma \ll \sigma_3$) a quadratic law is predicted and the $v(\sigma)$ curve becomes linear at high values of σ as the volume-diffusion step becomes rate controlling. Over a wide range of supersaturation values, Chernov's equation can be approximated by a law of the form

$$v \propto \sigma^{1.65}. \quad (4.48)$$

Gilmer, Ghez and Cabrera (1971) have given a more complete treatment of the mechanism of transport of solute particles to kinks in a step, including simultaneous volume and surface diffusion. They also assume a set of equidistant parallel steps and a high density of kinks so that diffusion along the edge of a step may be neglected. A single step of height h is considered at $y=0$, as in Fig. 4.17, and the volume and surface solute densities are related using three equations. Firstly, Fick's second law requires that, in the steady state,

$$\frac{\partial^2 n}{\partial y^2} + \frac{\partial^2 n}{\partial z^2} = 0 \quad (4.49a)$$

since diffusion in the crystal is neglected. Secondly, the surface-diffusion

FIG. 4.17. Step at $y=0$.

process as affected by the volume to surface flow is described by the equation

$$D_s \frac{\partial^2 n_s}{\partial y^2} + D \left(\frac{\partial n}{\partial z} \right)_{z=0} = 0 \quad (4.49b)$$

where n_s in this case is the surface concentration of solute per unit area. Finally, the exchange of solute between surface and volume is given by

$$D \left(\frac{\partial n}{\partial z} \right)_{z=0} = \frac{Dn}{\Lambda} - \frac{n_s}{\tau_{\text{deads}}} \quad (4.49c)$$

The factor D/Λ represents a "drift velocity" of solute molecules entering the adsorption layer from the adjacent volume such that $\Lambda = \lambda \tau_{\text{desolv}} / \tau_{\text{rdiff}}$ where λ is the mean free path in the solution and the τ 's are relaxation times for desolvation and volume diffusion.

The net exchange of solute at a kink is given by the net flux from neighbouring sites as

$$j = D \left(\frac{\partial n}{\partial y} \right)_{y=0} = \frac{D}{\Lambda_s} \left[(n_s)_{y=0} - n_e \right] \quad (4.50)$$

where $\Lambda_s = \lambda \tau_{\text{kink}} / \tau_{\text{sdiff}}$ is the quantity analogous to Λ for surface diffusion.

In the solution to these equations, the critical parameter is found to be $b = y_s / \Lambda$ where y_s is, as before, the mean distance travelled by an adsorbed solute molecule on the crystal surface. The growth rate in the limit $b = 0$ is given by

$$\frac{\rho v}{Dn_e} = \sigma \left[A + \delta + \frac{AA_s y_o}{y_s^2} + A \left\{ \frac{y_o}{2y_s} \coth \left(\frac{y_o}{2y_s} \right) - 1 \right\} \right]^{-1}. \quad (4.51)$$

This equation is analogous to Ohm's law in electricity, σ being the driving force for crystal growth and $\rho v/Dn_e$ a growth "current". Each of the terms in the square brackets has the character of an impedance. The first may be regarded as the impedance of the adsorption reaction and the second is that of the boundary layer. The third term represents an impedance for entering the steps and the fourth is that due to surface diffusion.

Equation (4.51) includes Chernov's theory and the BCF theory and reduces to these when the appropriate assumptions are made. The effect of a non-negligible value for b can be included only by numerical computation and examples of such calculations are given in the original paper. Results of computer simulation of crystal growth taking into account surface diffusion have been published by Gilmer and Bennema (1972).

It should be noted that, in this treatment, adsorption-controlled growth which would be expected for large values of A is linear in the supersaturation. This result conflicts with that of Reich and Kahlweit (1968) which is discussed in the next Section.

4.10. The Role of Desolvation

The formation of complexes between solute and solvent is well established, and the requirement of desolvation prior to growth has been discussed briefly in Section 4.5. Desolvation must occur at the crystal surface since the surface cannot provide a driving force for desolvation at long range. If, as in the Chernov and BCF solution-growth theories, solute were to enter the kink sites directly from the solution, desolvation would have to occur at the same time as the integration process. It appears reasonable to expect that adsorption onto the surface, which permits partial desolvation and orientation of the molecules prior to entry into a kink, will be a more probable mechanism.

This latter conclusion was reached by Davies and Jones (1951) who studied the precipitation of silver chloride from aqueous solution by monitoring the electrical conductivity of the solution. They reasoned that, if the growth kinetics were determined by the reaction of Ag^+ and Cl^- ions at the interface, the rate of crystallization would be proportional to n_{sn}^2 , where n_{sn} is the concentration of AgCl in the solution. Since this rate must equal the dissolution rate when $n_{sn} = n_e$, the net growth rate should be proportional to $n_{sn}^2 - n_e^2$. Experimentally they found that the rate of precipitation was proportional to $(n_{sn} - n_e)^2$, and this led them to reject a model in which adsorption was not included.

Doremus (1958) reviewed the experimental data on the precipitation

of relatively insoluble salts and also stressed the importance of an adsorption layer. In experiments where ions of one constituent were added in excess of the stoichiometric ratio, the rate of precipitation was found to be substantially unchanged on adding more of the excess ions. This result is best explained by assuming the existence of an adsorption layer which is "saturated" by the excess ions since the growth rate then depends only on the minority ion concentration. Doremus extended the concept of surface reaction-controlled growth, considering both the formation of molecules on the surface prior to diffusion to a kink and the separate surface diffusion of oppositely charged ions which are integrated alternately into the crystal at the kink sites. In the first case, the precipitation rate was calculated to be proportional to $(n_{se} - n_r)^3$ for a "one-one" electrolyte AB and to $(n_{sn} - n_r)^4$ for a "two-one" electrolyte A_2B . These dependences became $(n_{sn} - n_r)^2$ and $(n_{sn} - n_r)^3$ respectively for the latter model. Several examples of a cubic growth law were quoted.

Reich and Kahlweit (1968) proposed a theory which is related to the BCF volume diffusion theory but which should be applicable to those cases where desolvation at the kinks is the rate limiting kinetic process. According to their treatment, the rate of advance of steps is governed by the flux of desolvated ions to the kinks. The step velocity is given by

$$v_{st} = \frac{3V_m a^2}{\tau_{des} x_0} (n_{sn} - n_s) \exp(W_{des}/kT) \quad (4.52)$$

where τ_{des} is the relaxation time for desolvation at a kink and W_{des} the potential barrier for desolvation. At low supersaturations $v_{st} \propto \sigma$ through the term $(n_{sn} - n_s)$ and a parabolic $v(\sigma)$ law is expected since $y_0 \propto 1/\sigma$ as in the BCF theory. At high supersaturations volume diffusion will become the rate-limiting step as predicted in all treatments of solution growth.

4.11. Comparison of Solution Growth Theory with Experiment

One spectacular success of the BCF theory is that it successfully predicted the occurrence on crystal surfaces of growth spirals, which have now been observed on a wide variety of crystals. In this section we examine the ability of this theory and its various extensions to account for experimental determinations of the variation with supersaturation of the growth rate of crystals from solution.

In interpreting experimental data, difficulty is frequently encountered in distinguishing between boundary-layer and interface-kinetic effects. Two methods are available for obtaining the form of the $v(\sigma)$ relationship for the kinetic process by experiment. The first is to measure the variation of growth rate with solution flow rate or crystal rotation rate and to extract

the $v(\sigma)$ relationship using Eqn (4.21). Alternatively, high flow rates or rotation rates may be used and the assumption made that the growth rate is then controlled only by the interface kinetics. The latter assumption is often of dubious validity and experimental data may underestimate the true kinetic-controlled growth rate because no allowance is made for a desolvation or minimum diffusion stage. Unfortunately data obtained by either method are not available for growth on a habit face from high-temperature solution and we therefore consider the results of experiments on aqueous solutions. (Measurements of the growth rate in LPE experiments as a function of the substrate rotation rate will be described in Chapter 8.)

For those crystals to which Brice's method is applicable, that is for which the $v(\omega)$ or $v(u)$ data yield a straight line when plotted according to Eqn (4.21), a quadratic growth law is often found. Brice (1967a) used the experimental data on sucrose (van Hook, 1945) and $\text{CuSO}_4 \cdot 5\text{H}_2\text{O}$ (McCabe and Stevens, 1951; Hixson and Knox, 1951) and found that $v \propto \sigma^2$ except for Hixson and Knox's data above 71°C , which indicated a linear growth law. The data of Coulson and Richardson (1956) also fit a quadratic law but our attempts to apply Eqn (4.21) to the results of other investigators were not successful. For example, the data of Mullin and Gaska (1969) yield a highly non-linear plot of $vu^{-1/2}$ against $v^{1/2}$ although the growth rates at high values of u indicate a quadratic law. The extent of the discrepancy between these values and Eqn (4.21) is indicated by an increase of $vu^{-1/2}$ with v , a similar discrepancy with Eqn (4.21) being also found for citric acid using the data of Cartier *et al.* (1959). This discrepancy may be due to convective flow in the solution.

A quadratic growth law has been found for a number of materials grown under conditions of rapid flow. Examples are sodium chloride (Rumford and Bain, 1960), ammonium dihydrogen phosphate (ADP) and potassium dihydrogen phosphate (KDP) (Mullin and Amatavivadhana, 1967) and potassium sulphate (Mullin and Gaska, 1969). However, a linear growth law has been discovered by Bransom *et al.* (1949) for the growth of cyclonite, by Belyutsin and Dvoryakin (1957) for various alums and by Bennema (1966b) for potassium aluminium alum.

Discrepancies are frequently noted between the results of different investigators. For example, Mullin and Garside (1967) found that their results for potassium aluminium alum are best described by a curve of the form $v \propto \sigma^{1.62}$, which is in agreement within experimental error with the expression given by Chernov (Eqn 4.48). The discrepancy between their results and those of Bennema may be due to the higher supersaturation range studied by Mullin and Garside. Chernov's theory is also supported by the data of Kunisaki (1957) on ethylene diamine tartrate and by

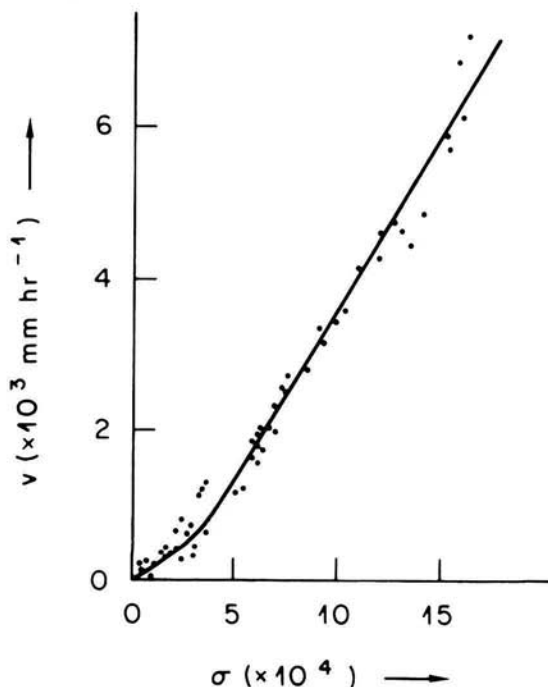


FIG. 4.18. Growth rate of sodium chlorate (after Bennema, 1967).

Garabedian and Strickland-Constable (1970), who reported a variation of the form $v \propto \sigma^{1.73}$ for the growth of sodium chlorate.

Bennema (1967) used his own results on sodium chlorate to support his case for the inclusion of surface diffusion in crystal growth from solution. The experimental data are shown in Fig. 4.18 together with a curve plotted using the BCF surface-diffusion formula, Eqn (4.41). A similar curve would be predicted by the BCF volume-diffusion theory but in that case the linear region would be controlled by boundary-layer diffusion. Bennema found, however, that changing the stirring rate had no effect on the crystal growth rate and was therefore confident that the measured growth rate was determined by the interface kinetics. The slope in the linear region is roughly one tenth that expected for volume-diffusion control (Eqn 4.14). This discrepancy was given an alternative explanation by Gilmer *et al.* (1971) by the inclusion of the parameter Λ which appears in Eqn (4.51). Then, in the linear region,

$$\frac{dv}{d\sigma} = \frac{Dn_c}{\rho(\delta + \Lambda)} \quad (4.53)$$

from which they estimate $\Lambda \approx 10\delta \approx 0.1$ cm in this case. The data of Garabedian and Strickland-Constable clearly do not agree with those of Bennema but, again, this may be due to the fact that they were obtained at much higher supersaturations.

Alexandru (1971) investigated the growth of ADP by a method similar to that used by Bennema and also found that his results were best explained by the BCF surface-diffusion theory.

Gilmer *et al.* (1971) used Eqn (4.51) to interpret data of Smythe (1967) on the growth of sucrose crystals. A linear dependence of τ on σ was observed by Smythe at temperatures from 20°C to 70°C. The value of Λ at 21°C is estimated as 2×10^{-2} cm, which is much larger than the estimated value of $\delta = 4 \times 10^{-4}$ cm. If this interpretation is correct, the growth mechanism must involve adsorption followed by surface diffusion since Λ represents the effective impedance of the adsorption process.

When the results on precipitation, described in the last section, are included, the weight of evidence appears to favour a growth mechanism which includes a surface-diffusion process in many cases. This conclusion is supported by estimates by Conway and Bockris (1958) of the energy changes occurring during electrocrystallization. They concluded that the energy required to transfer an ion to a surface site is much less than that for direct transfer to a kink, and therefore favoured an initial surface adsorption stage. Electrocrystallization must, of course, include the transfer of an electron which is required before an ion in the solution can become a neutral atom, but the situation is otherwise identical to crystal growth from solution.

The number of $\tau(\sigma)$ measurements on crystals grown from high-temperature solutions is very small, and these have been made only on unstirred solutions.† Elwell and Dawson (1972) found a linear variation for the growth of nickel ferrite from barium borate and of sodium niobate from NaBO_2 . The data for nickel ferrite are shown in Fig. 4.19, and growth in this case is believed to be controlled by volume diffusion through the boundary layer. The value of D/δ calculated using Eqn (4.14) is found to be 5.7×10^{-4} cm s⁻¹. The value of δ estimated from Eqn (4.17) using $\eta \approx 20$ cP, $\rho_{s,u} \approx 4.5$ g cm⁻³, $D \approx 10^{-5}$ cm² s⁻¹, $u \approx 0.1$ cm s⁻¹ and $l = 0.5$ cm is $\delta \approx 0.06$ cm, which gives $D/\delta \sim 1.6 \times 10^{-4}$ cm s⁻¹. The agreement between theory and experiment is as good as can be expected in view of the uncertainties in the values of D , η and u .

A quadratic $\tau(\sigma)$ variation was found for the growth of barium strontium niobate $\text{Ba}_{0.5}\text{Sr}_{0.5}\text{Nb}_2\text{O}_6$ from the system $\text{BaO}-\text{SrO}-\text{Nb}_2\text{O}_5-\text{B}_2\text{O}_3$ as shown in Fig. 4.20. A remarkable feature of these results is the persistence

† Measurements on stirred solutions will be published in *J. Crystal Growth* by Elwell, Capper and D'Agostino.

of the quadratic law to supersaturations of up to 10%. A critical supersaturation σ_1 of 10% is two orders of magnitude greater than the highest value reported by Bennema (1967) for crystal growth from aqueous solution although Bennema *et al.* (1972) recently revised their estimate of σ_1 to $\sim 10^{-1}$. According to Eqn (4.40), σ_1 is given by $9.5\gamma_m a/kTy_s$, so that a high value of σ_1 requires either a high value of γ_m or a low value of y_s . A high value of σ_1 thus appears to be unfavourable for crystal growth since both low y_s and high γ_m will favour desorption of surface molecules rather than integration into the kinks, and it is found experimentally that $\text{Ba}_{0.5}\text{Sr}_{0.5}\text{Nb}_2\text{O}_6$ is a difficult material to crystallize from borate solvents. The quadratic law may also be due to a surface reaction between, say, BaNb_2O_6 and SrNb_2O_6 units, as suggested by Tiller (1971), but current knowledge of the ionic species present in the solution is insufficient to allow any firm conclusion. A quadratic $v(\sigma)$ variation was found to explain the growth-rate measurements of NaNbO_3 from a NaBO_2 flux (Dawson *et al.*, 1974) and of $\text{KTa}_{1-x}\text{Nb}_x\text{O}_3$ from a K_2CO_3 flux (Whiffin and Brice 1974).

Newkirk and Smith (1965) observed a linear variation in the growth of BeO from a number of $\text{Li}_2\text{O}/\text{MoO}_3$ solvents. The growth rates for this

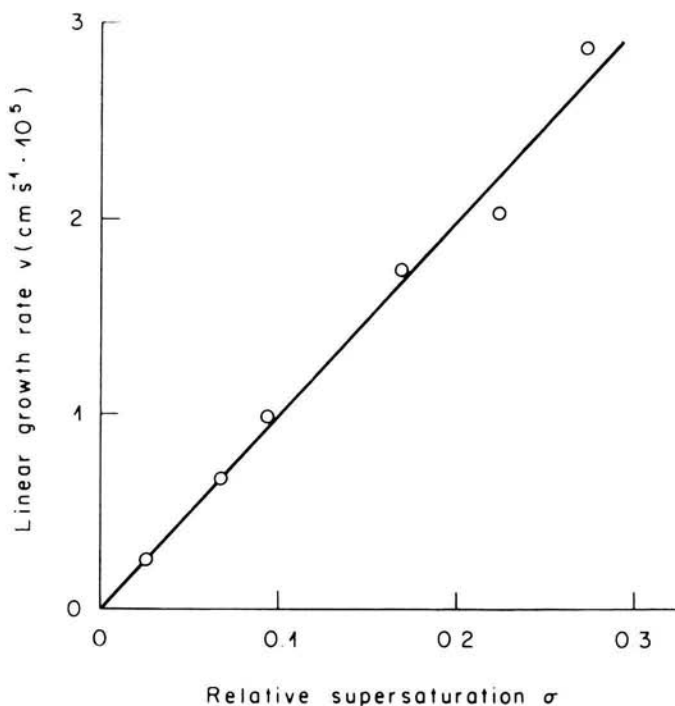


FIG. 4.19. Growth rate of nickel ferrite (Elwell and Dawson, 1972).

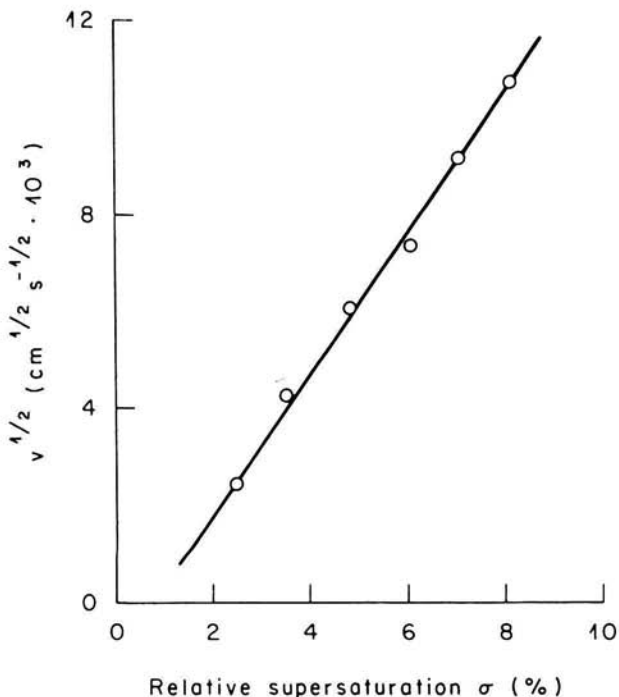


FIG. 4.20. Growth rate of barium strontium niobate (Elwell and Dawson, 1972).

material were only of the order of $10^{-8} \text{ cm s}^{-1}$, some 2 orders of magnitude lower than those shown in Figs 4.19 and 4.20, which are more typical of the maximum values possible in high-temperature solution growth (Scheel and Elwell, 1972, 1973a). It is unlikely that such low growth rates for BeO can be explained simply by a low coefficient of volume diffusion, and the simplest explanation would be to postulate a high value for the adsorption parameter of Gilmer *et al.* (1971). (It was mentioned above that a linear $v(\sigma)$ relation is difficult to explain in terms of the BCF surface-diffusion theory when the back-stress effect is included. In the next section we shall discuss the shapes of spirals which may be expected to result when the growth centre is a pair or group of spirals; one example which can result in a linear $v(\sigma)$ variation will be included.)

4.12. Non-Archimedean Spirals

In the previous discussion the growth spirals have been assumed to be of approximately Archimedean shape and to have their origin in a single dislocation with a screw component. Frequently, however, dislocations occur in pairs or groups and the spirals originating from such centres will

normally have more complex shapes, and the growth mechanism may differ from the simpler case considered in Section 4.7.

If the growth centre is a pair of dislocations of like sign, separated by a distance greater than $2\pi r_s^*$, the shape of the resulting spiral will have the form shown in Fig. 4.21. If the crystal face is divided as shown by the heavy dashed line, which will be slightly curved, the two sections will be fed with steps from the two centres, respectively. The activity is approximately the same as that of a single spiral. When the centres are separated by less than $2\pi r_s^*$, the arms of both spirals reach the whole area; if the separation is much less than r_s^* , the centre effectively generates two spirals, each with the same step velocity, and so the activity of the centre will be twice that of a single dislocation.

When a pair of dislocations of opposite sign are separated by a distance greater than $2\pi r_s^*$, the steps join up to form closed loops, as shown in Fig. 4.22. This type of cooperation in which a screw-dislocation source generates a series of continuous layers has been observed by Forty (1951) and Griffin (1951), along with many other examples of spirals due to interacting dislocations.

If there are two similar pairs of dislocations separated by a distance large compared with the separation in each pair, the steps will combine on meeting and the number of steps passing any point on the surface will be the same as if only one pair existed. Generalizing from this statement, the growth rate of a face containing several pairs of dislocations of opposite sign will be the same as that of a face having only one such pair as the

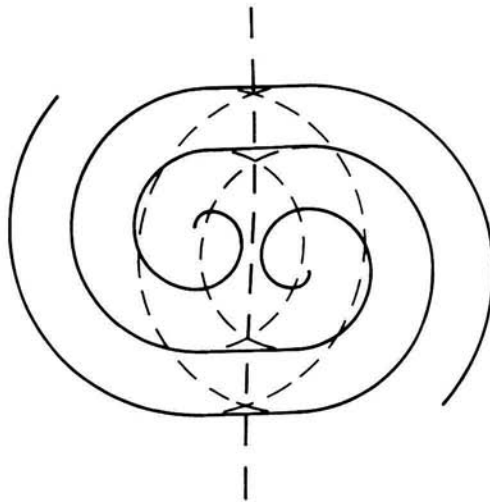


FIG. 4.21. Growth spiral due to pair of dislocations of like sign.

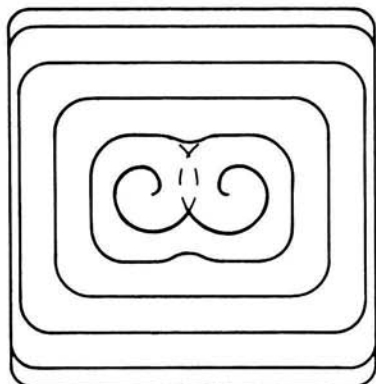


FIG. 4.22. Layers due to a pair of dislocations of opposite sign.

active centre. When the separation of a pair is less than $2r_s^*$, step motion cannot occur and so no growth will proceed from such a centre.

An interesting case arises when a group of dislocations of the same sign, all separated by the same distance smaller than $2\pi r_s^*$, acts as a spiral source. Such an array of dislocations may form wherever screw dislocations occurring in a group lie along some line. The type of spiral produced by this type of group is shown in Fig. 4.23. The separation y_0 of the spirals generated will be determined by the separation l between the dislocations and is thus independent of the supersaturation σ . As a result, the growth rate $v(=v_{st} a/y_0)$ will depend on the supersaturation only through the term v_{st} . Since $v_{st} \propto \sigma$ [Eqn (4.37)], a linear $v(\sigma)$ law is expected and this may explain the experimental observation of linear kinetic laws for some materials.

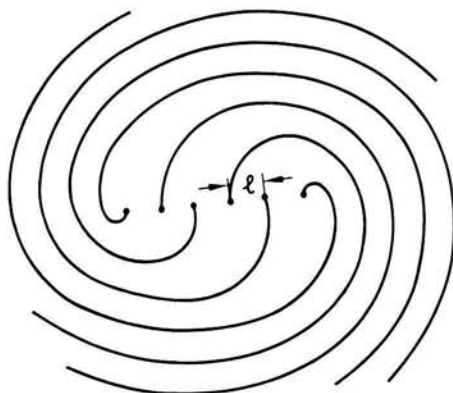


FIG. 4.23. Spiral due to a group of dislocations lying along a line.

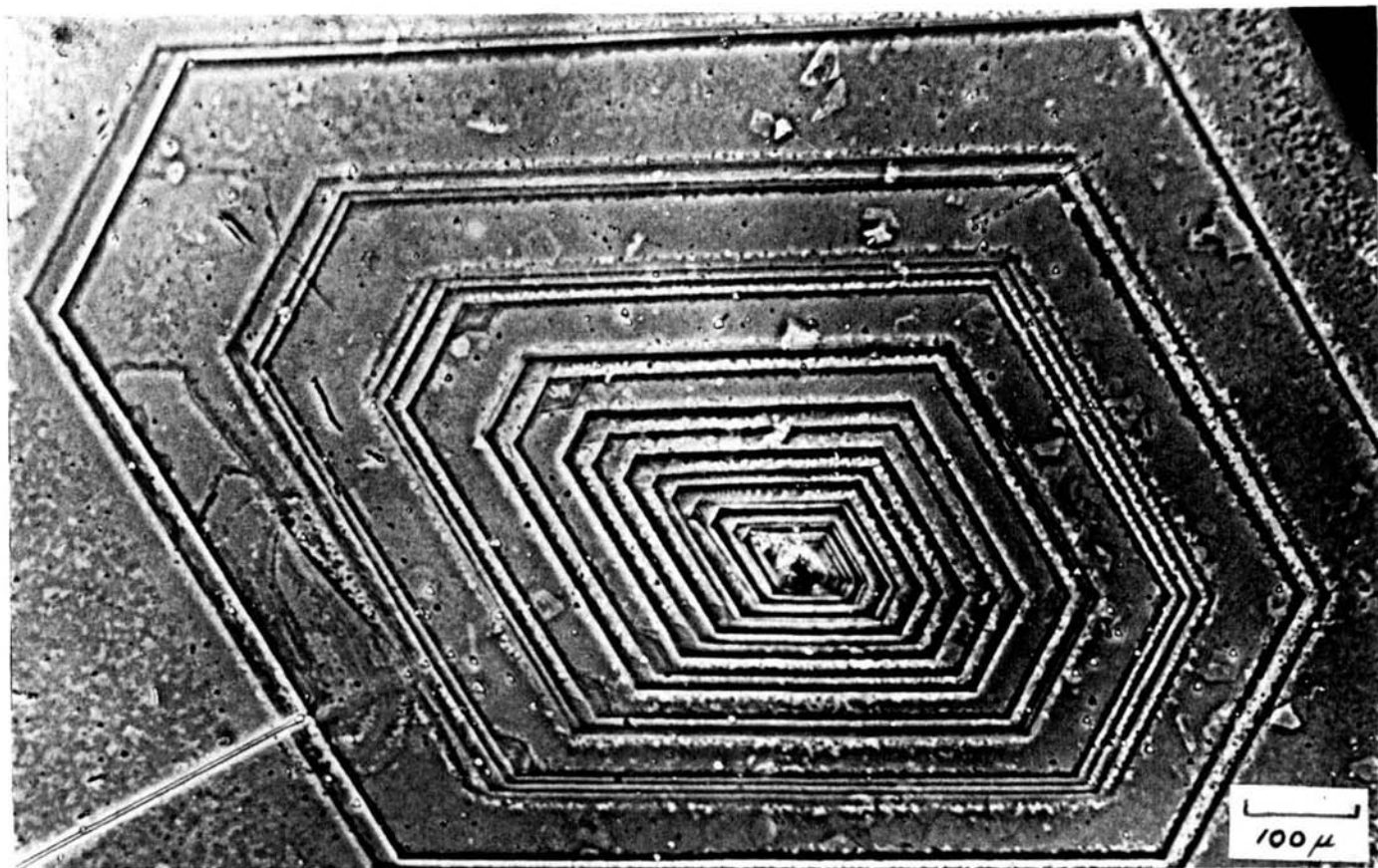


FIG. 4.24. Spiral on barium zinc ferrite (after Cook and Nye, 1967).

Frequently the spirals which are observed experimentally do not have curved edges. If the rate of advance of a step over a crystal surface depends upon the orientation, the spiral may readily develop straight edges which are related to the slow-growing faces of the crystal. An example of such a "polygonized" spiral is shown in Fig. 4.24. This spiral was observed (using optical microscopy) by Cook and Nye (1967) on a flux-grown crystal of $\text{Ba}_2\text{Zn}_2\text{Fe}_{12}\text{O}_{22}$. The spiral is on the basal plane of the crystal and its shape clearly reflects the hexagonal symmetry normal to this plane. The height of the steps in some spirals was determined by replication electron microscopy as 14.5 \AA , which corresponds to the unit-cell edge.

The spirals and growth features which are observed experimentally are often not of unit-cell dimensions but may be built up of 100–10000 unit cells. In a review by Honigmann (1958), surface studies on solution-grown crystals of eleven different materials were reported. Spirals were observed on seven of these materials and non-spiral layer growth on eight. On six materials, the steps were of one or two unit cells in height, on three they were of many unit cells in height and on two, step heights in the region of 1000 \AA were observed.

The formation of "macrospirals" observable with a simple microscope

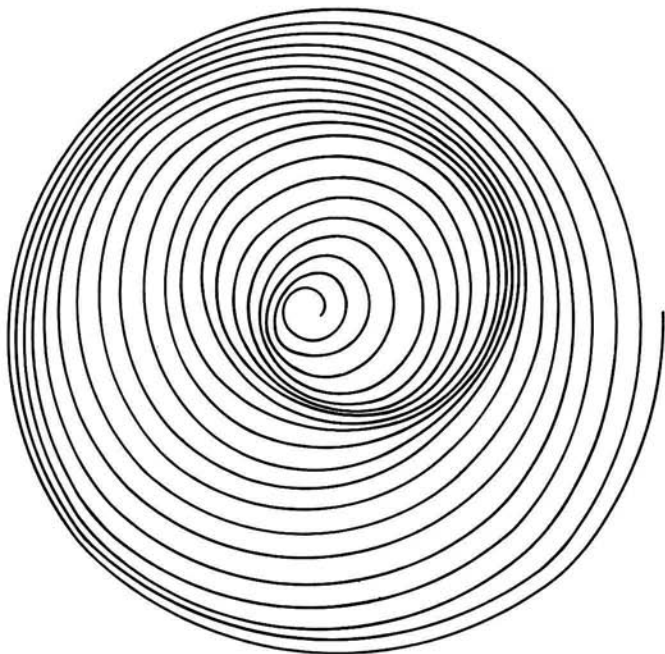


FIG. 4.25. Macrospiral formation due to periodic motion of centre.

was explained by Amelinckx, Bontinck and Dekeyser (1957) as being due to a "wobbling" of the centre of the spiral at a helicoidal screw dislocation. The effect of a periodic perturbation of the spiral centre is illustrated in Fig. 4.25, in which the regular fluctuation in the pitch of the spiral may be seen to give the impression of a spiral of greater pitch. The periodic perturbation can be included in the theory by replacing the factor ϵ in Eqn (4.44) by $\epsilon_0 \sin \omega t$, so that

$$z(t) = \frac{C\epsilon_0 \sin \omega t \sigma^2}{\sigma_1} \tanh \frac{\sigma_1}{\epsilon_0 \sin \omega t \sigma}$$

and the appearance of a macrospiral will be governed by the relative magnitudes of the frequency ω of the perturbation and the frequency of rotation of the spiral. Bennema and van Rosmalen (1972) have shown that fluctuations will always reduce the flow of steps σ_1 and therefore the rate of growth.

Bennema (1969) has argued that polygonization of the macrospirals is explained more readily if surface diffusion of solute occurs than if solute enters the kink sites directly. He considered in particular the observations of Torgeson and Jackson (1965) of the macrospiral shapes on ADP crystals grown from aqueous solution. When the crystals are grown in a pure solution, the macrospirals on (100) faces are elliptical with a shorter axis in the [001] direction as shown in Fig. 4.26(a). When Cr^{3+} ions are added to the solution, the spirals become polygonized along [010] and [001] directions as shown in Fig. 4.26(b).

According to the PBC description of Hartman (1956), the {100} surfaces

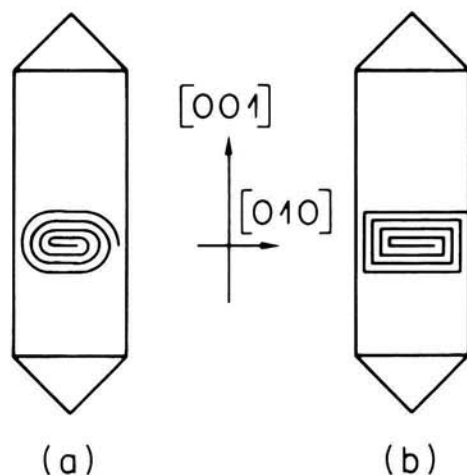


FIG. 4.26. Macrospirals on ADP, schematic (after Torgeson and Jackson, 1965).

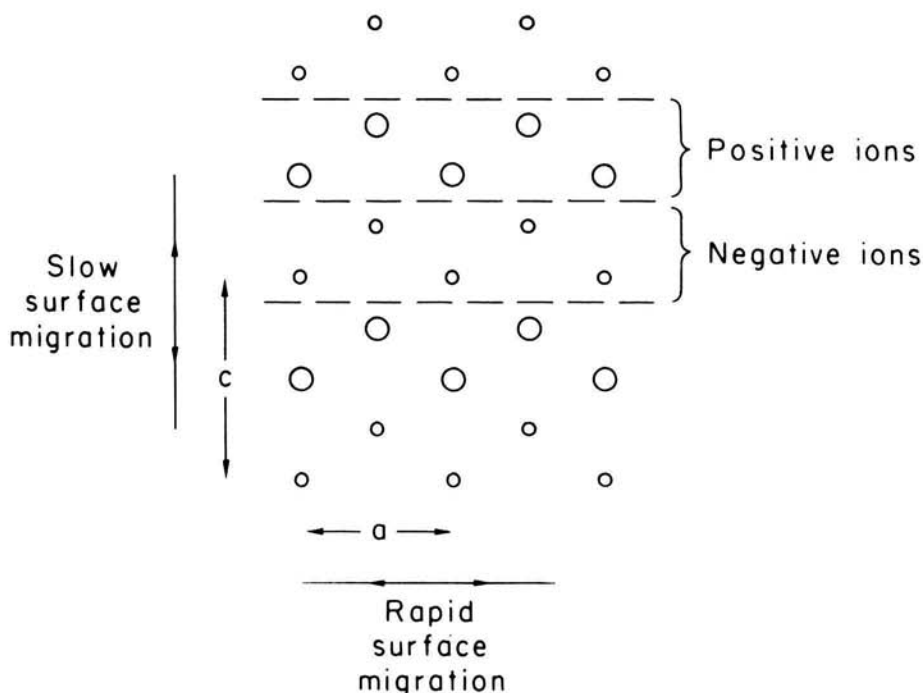


FIG. 4.27. Structure of ADP surface (after Hartman, 1956).

of ADP can be considered as narrow regions of positive ions extending in the $[100]$ direction with a width of $c/2$, alternating with similar regions of negative ions as shown in Fig. 4.27. An ion in the surface can diffuse relatively easily along the $[010]$ direction since it always moves past ions of the same sign. Migration along $[001]$ is, however, relatively difficult since alternate layers are of opposite charge. This difference in surface-diffusion rates along $[010]$ and $[001]$ accounts for the ellipticity in the spiral of Fig. 4.26(a).

When Cr^{3+} ions are added to the solution, many of the kink sites are filled preferentially with these ions so that the number of kink sites available for growth is reduced. Polygonization results from the retardation in the rate at which steps can advance across the surface, but the anisotropy in the spiral shape is preserved since surface diffusion remains anisotropic. While alternative means of explaining these results could be considered (see Section 5), an anisotropic surface-diffusion mechanism appears to offer the simplest explanation.

Although macrospirals are observed quite frequently on crystal surfaces, a quantitative theory of their development is still lacking. A qualitative

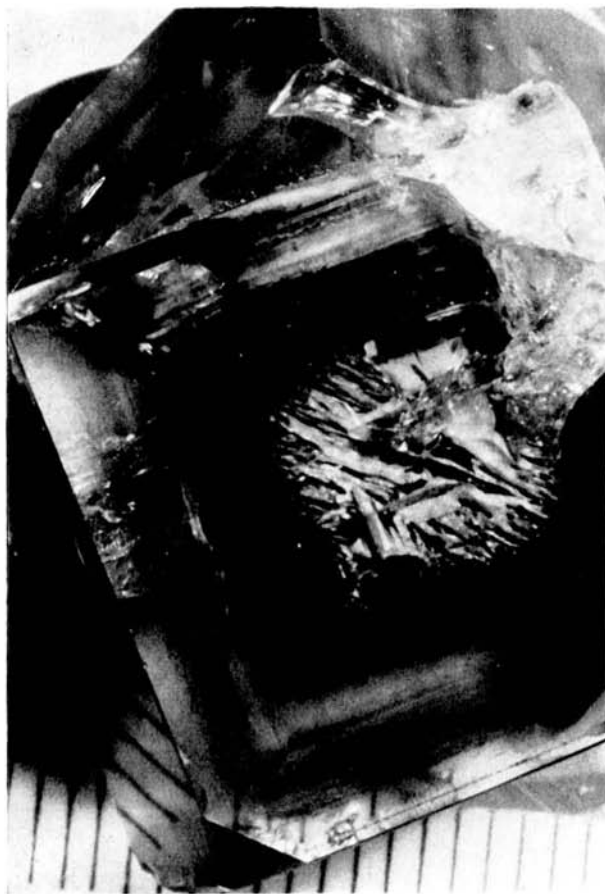
treatment of the "bunching" of steps has been given by Cabrera and Vermilyea (1958) and by Frank (1958b) based on the kinematic wave theory of Lighthill and Whitham (1955). The formation of large steps by bunching is governed by kinetics rather than by thermodynamics. The velocity of any step depends on the proximity of other steps, which will remove some of the solute. The rate of flow of steps will therefore depend on the average separation between steps and the kinematic wave theory describes the motion of macrosteps of constant separation at some rate v'_m which is less than the velocity v_s of a single step. Bunching will be particularly likely to occur if the velocity v'_m is increasing as crystal growth continues, since in this case newly formed steps will tend to overtake those already present on the surface. Bunching is also more probable in impure solutions, since impurity molecules which are rejected by the crystal interface tend to impede the motion of steps; highly immobile impurity ions may become incorporated into the crystal at the resulting macrosteps. Also the solution flow rate might have an effect on the average step height.

4.13. Surface Morphology of Flux-grown Crystals

Reference has been made above to the observation of growth spirals on the surfaces of orthoferrite crystals by Tolksdorf and Welz (1972) and of polygonized spirals on hexagonal ferrites by Cook and Nye (1967). These observations and the earlier ones of Sunagawa (1967) and others support the validity of Frank's screw-dislocation model. In this section we consider other observations of surface features of crystals grown from high-temperature solutions and the relation between these features and the mode of growth. A more extensive discussion of this topic has been given by Chase (1971).

When crystals nucleate in solution, the supersaturation is normally much higher than that at which the subsequent growth occurs. As a result the initial growth of spontaneously nucleated crystals tends to be highly dendritic. The dendrites grow along fast growth directions and this rapid growth reduces the supersaturation. Subsequent growth occurs more slowly but the ends of the dendrites will be located in regions of higher supersaturation than the central region, and solvent inclusions are trapped near the growth centre as the dendrite arms close. An initial dendritic growth stage has been described by several authors, for example Lefever and Chase (1962), White (1965), Chase (1968) and Scheel and Schulz-Dubois (1971). Figure 4.28(a) shows a large crystal of $GdAlO_3$ in which the central dendritic region may be clearly seen, and Fig. 4.28(b) shows the same crystal in reflected light with the large concentration of growth hillocks in the region above the dendritic core.

As growth proceeds on the dendritic core, the stepped edges of the



(a)



(b)

FIG. 4.28. (a) Dendritic centre of $GdAlO_3$ with flux inclusions; (b) effect on growth hillocks (reflection photograph Scheel and Elwell, 1973b).

dendrite arms provide sites for the integration of solute and a terraced structure is produced. If growth is terminated at this stage the crystals are found to exhibit a "hopper" morphology as illustrated in Fig. 4.29. The mechanism of hopper formation was discussed by Lefever and Giess (1963), who pointed out that hopper crystals will be more likely if the initial dendrites attain large dimensions and so incorporate a large fraction of the available solute.

According to Scheel and Elwell (1973a) hopper growth is assumed to be an effect of unstable growth. By increasing the supersaturation gradient, increasingly unstable growth in the following sequence will occur: flat faces \rightarrow formation of inclusions \rightarrow edge nucleation \rightarrow hopper growth \rightarrow dendritic growth.

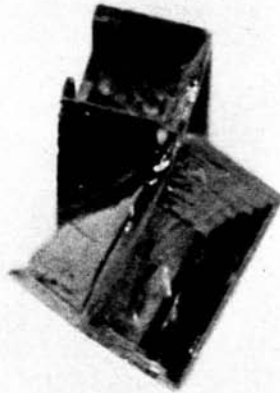
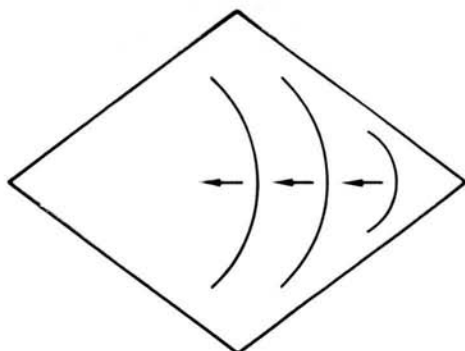
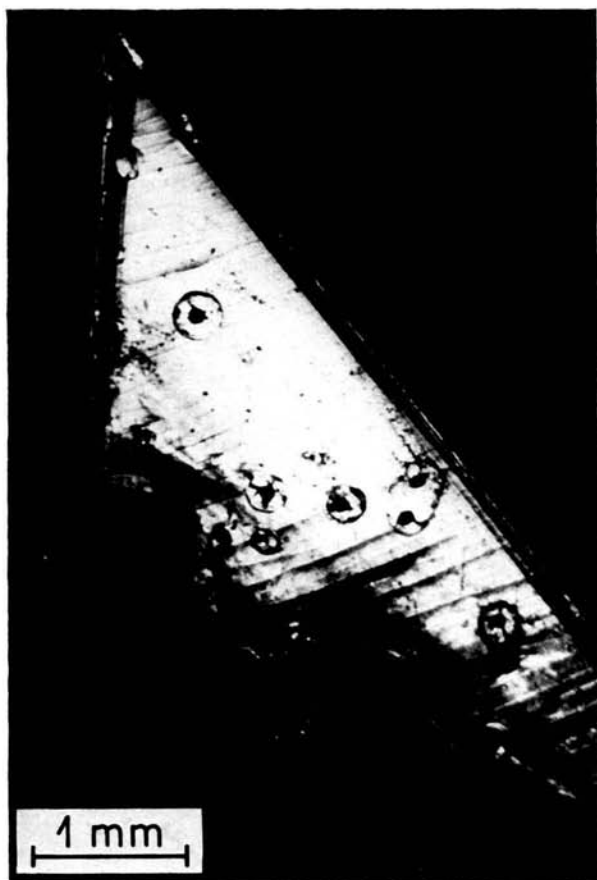


FIG. 4.29. Hopper crystal of hematite (courtesy Mrs. B. M. Wanklyn).

An alternative mechanism of hopper formation was proposed by Amelinckx (1953). The crystals in this case were considered to grow while floating on the solution so that the centre of the face is not in contact with the supersaturated solution. Since contact with the solution occurs only at the edge, growth occurs only where a step in the growth spiral meets an edge and a narrow strip of material is deposited. This strip continues to grow along the edge of the crystal and a vertical hollow box would tend to develop except that the crystal simultaneously grows laterally. Each turn therefore appears at a greater lateral distance from the centre than the previous one and the characteristic terraced depression develops. In the extreme case of growth at the edges of a crystal, the resulting shape will be a hollow rectangular tube.



(a)



(b)

FIG. 4.30. Layer growth nucleated at edges and corners. (a) diagrammatic, (b) edge nucleation on β -eucryptite, LiAlSiO_4 (courtesy K. Meyer, ETH Zurich).

If all the crystal faces remain in contact with the solution, continued growth will eventually result in the establishment of the habit faces. Growth at relatively high temperatures (and presumably at rather high supersaturation) was found by Lefever and Chase (1962) to proceed by nucleation of layers at corners or edges of the garnet crystals studied. The layers in this case were normally curved in a direction concave from the point of origin, as shown in Fig. 4.30(a). This curvature arises because of the higher supersaturation at corners and edges which can lead to an increase of growth rate with distance from the centre of the face. Similar layers were observed by Chase (1968) on In_2O_3 crystals and by Quon and Sadler (1967) on yttrium iron garnet. In the latter case a similar structure made up of much finer layers was also observed. An example of edge

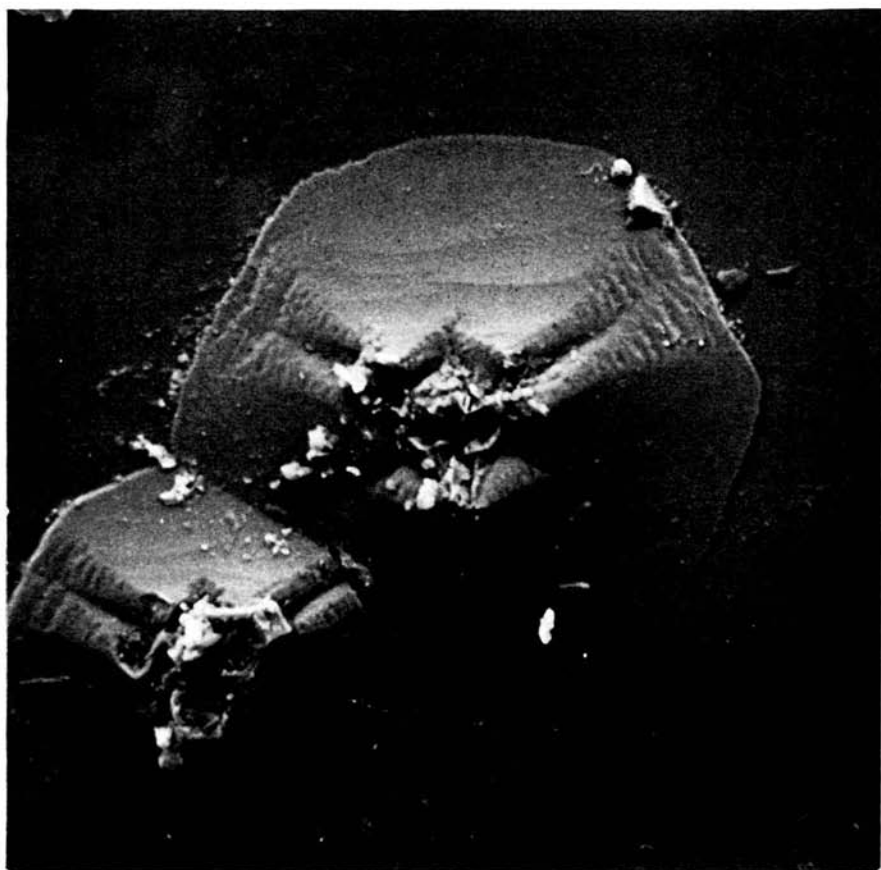


FIG. 4.31. Growth hillocks on nickel ferrite (Elwell and Neate, 1971).

nucleation on a β -eucryptite (LiAlSiO_4) crystal grown from a vanadate flux is shown in Fig. 4.30(b).

If the supersaturation is lowered below the value which can promote corner and edge nucleation, the characteristic features seen on most crystals are growth hillocks, consisting of layers roughly 10^{-5} cm in height. Typical hillocks are illustrated in Fig. 4.31. Growth hillocks are presumably formed by a bunching process, as described in the previous section, which gives rise to the relatively thick layers visible under the microscope. Other examples of growth hillocks have been described by Lefever and Chase (1962) and Quon and Sadler (1967) on garnets, by Chase (1968) on In_2O_3 , by Sunagawa (1967) on aluminium oxide and by Scheel and Elwell (1973b) on rare-earth aluminates. Sunagawa (1967) has



FIG. 4.32. Triangular growth layers on lithium ferrite (Elwell and Neate, 1971).

investigated a large number of flux grown crystals and has observed spirals of monomolecular step height on magnetoplumbite, $\text{PbFe}_{12}\text{O}_{19}$, on ferric oxide, alumina and yttrium iron garnet. Pyramidal layers were observed on spinel, MgAl_2O_4 . The number of features seen on a given face appears to depend on the supersaturation and a single feature often dominates a whole face when growth occurs at low supersaturation. This decrease in the number of active centres as growth proceeds may have an influence on the maximum rate of stable growth, as is discussed in Chapter 6.

Triangular growth layers were observed by Elwell and Neate (1971) on ferrite crystals, an example being shown in Fig. 4.32. This feature appeared to be the only active growth centre on that particular face, and the layer height ($\sim 10^{-5}$ cm) is clearly determined by some bunching effect. A mechanism of crystal growth by the spreading of layers of similar height was reported by Bunn and Emmett (1949) who studied the growth of lead nitrate from aqueous solution.

As discussed earlier in the chapter, layers, hillocks and macrospirals may all have their origin in screw dislocations. Confirmation of the dislocated nature of hillock centres was reported by Lefever and Chase (1962), who found on etching the crystal surfaces that an oriented etch pit was formed at the centre of each hillock. The most likely conclusion to be drawn from these surface studies is that growth on habit faces at low supersaturation frequently occurs by the Frank screw-dislocation mechanism but that edge nucleation may be dominant at higher supersaturations.

4.14. Alternative Growth Mechanisms

Although the mechanism by which crystals grow from fluxed melts is often the BCF screw-dislocation mechanism, alternative growth mechanisms are not rare (Scheel and Elwell, 1973b).

Nucleation of surface layers at corners or edges of a crystal may be by 2-D nucleation rather than at screw dislocations. The relative ease of nucleation at corners or edges was first proposed from binding energy considerations by Stranski (1928). Corner and edge nucleation will clearly be favoured because of the relatively high concentration of solute in these regions, even if growth occurs by the screw-dislocation mechanism. Figure 4.33 shows an optical reflection micrograph of a GdAlO_3 crystal in which the concentration of hillocks is higher at the crystal edges due to the higher local supersaturation. As growth continues at a stable rate, the concentration of hillocks near the edges decreases and so edge growth becomes less important. The tendency of crystals to grow with raised edges is, however, favoured if growth becomes unstable, as will be discussed in Chapter 6.

A particularly powerful nucleation site may be formed when the faces



FIG. 4.33. Growth hillocks at edges and on faces of a GdAlO_3 crystal (Scheel and Elwell, 1973b).

of a twinned crystal meet along the twin plane at an acute angle. The resulting twin-plane re-entrant edge (TPRE) growth mechanism can be envisaged with reference to Fig. 4.34, which shows a section through a twinned crystal. The crystal grows by the propagation of layers in the directions indicated by v_L , and rapid growth may also occur in the direction of the twin plane, depending on the nature of the twin and the crystal structure.

The TPRE mechanism and its influence on the habit of crystals was described by Niggli (1920) and Spangenberg (1934), who both refer to Mügge (1911) and Becke (1911), by Wagner (1960), John and Faust (1961) and Faust and John (1964), the latter giving an extensive list of semi-

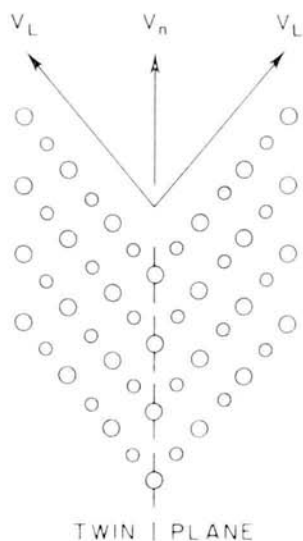


FIG. 4.34. Twin-plane re-entrant edge growth mechanism.



FIG. 4.35. Layer spreading influenced by multidomain twinning of NdAlO_3 (Scheel and Elwell, 1973b).



FIG. 4.36. Detail of interactions of twin domains and growth layers on NdAlO₃ crystal (Scheel and Elwell, 1973b).

conductors grown by this mechanism. The habit of Al_2O_3 , BeO and BaTiO_3 is controlled by the relative importance of this mechanism as will be discussed in the next Chapter.

Twin domains formed due to a phase transition during growth may affect the growth mechanism even when the angular deviation between twins is very small. Figures 4.35 and 4.36 show growth layers on the surface of neodymium-aluminate crystals. The pattern of layers is very closely related to the domain structure, although the twinning angle is less than 1° (Geller and Bala, 1956). This interrelation between growth layers and domains is not observed in crystals such as BaTiO_3 in which the domains are formed at temperatures well below the growth temperature.

It is not clear whether twin boundaries at very low angles act by



FIG. 4.37. Growth hillocks along a twin plane of GdAlO_3 (Scheel and Elwell, 1973b).



FIG. 4.38. Layers spreading from multiple twinned region of GdAlO_3 (Scheel and Elwell, 1973b).

providing centres for classical nucleation or because of a high concentration of screw dislocations. In some cases, the twin planes provide centres for the formation of growth hillocks as shown in Figs. 4.37 and 4.38. These photographs are of GdAlO_3 crystals, and examples have also been observed where twinned regions do not provide the dominant growth centres because of the presence of very active screw-dislocation sources (see Fig. 4.39).

Carlson (1958) proposed that low-angle grain boundaries may also provide more active growth centres than those due to isolated screw dislocations. Twist boundaries will give rise to screw dislocations, the separation of which is given by Nabarro (1967) as

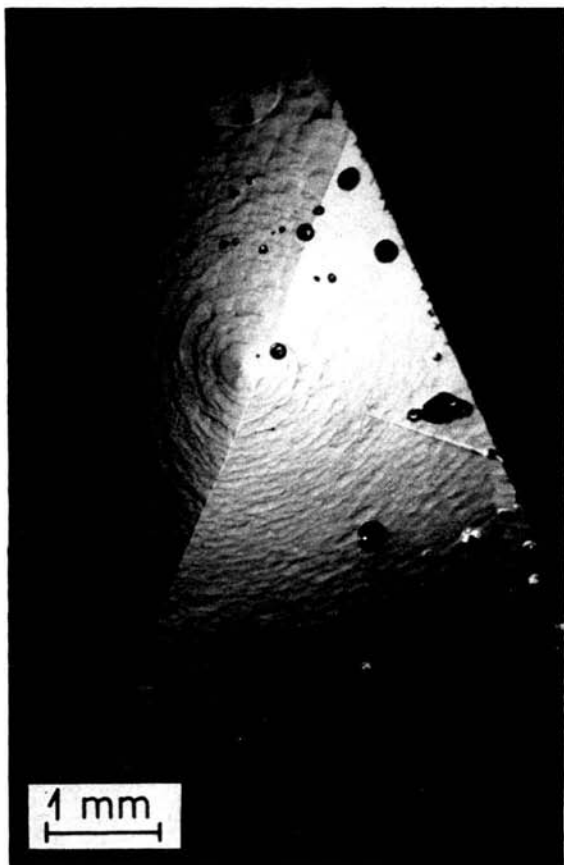


FIG. 4.39. Dominating growth centre near a twin plane of GdAlO_3 (Scheel and Elwell, 1973b).

$$d = \frac{a}{2} \operatorname{cosec} \phi/2$$

where a is the interatomic separation and ϕ the angle between the adjacent grains. Using the criterion of BCF for the cooperation between screw dislocations of like sign, that $d < 2\pi r^*$, the minimum angle for preferential growth at screw dislocations is given by

$$\sin \phi/2 > a/4\pi r^*.$$

Thus for $r^* \sim 20a$, (see Eqn (4.25a) with $\gamma_m/kT \sim 1$ and $\sigma = 0.05$), ϕ must be of the order of $1/2^\circ$, which is typical of the values at which a twin plane acts as the dominant growth centre.

Cracks which develop in any crystal due to severe strain during growth



FIG. 4.40. Growth along crack of a GdAlO_3 crystal (Scheel and Elwell, 1973b).

provide many active growth centres and tend to "heal" by relatively rapid local growth. Figure 4.40 shows a GdAlO_3 crystal in which a crack has developed during removal of the crucible from the furnace in order to pour off the residual solution. The crack has clearly resulted in many growth centres which were more active than centres which had previously dominated growth over the whole face.

In any attempt to assess the growth mechanism of a crystal, care must be exercised to allow for the mutual influence which neighbouring faces exert upon each other. An example of this influence is shown in Fig. 4.41 which shows two faces of GdAlO_3 inclined at 90° to each other. Layers on the two faces run in opposite directions, and the layer-rich regions of the two faces correspond to each other. On some crystals one face had very



FIG. 4.41. Two adjacent faces (at nearly 90°) of GdAlO_3 (Scheel and Elwell, 1973b).

active growth centres, with adjacent faces showing hardly any features, suggesting that the latter faces grew by edge nucleation from the more active face. Such observations are contrary to the PBC concept, which treats all $\{100\}$ faces of a pseudocubic perovskite as essentially equivalent, and indicate that generalizations on growth mechanisms should be expressed with care.

4.15. Summary

(i) The rate of nucleation of crystals varies rapidly with supersaturation once a critical value, of the order of 10^0 , is exceeded and is very low at lower supersaturations.

(ii) The initial growth following spontaneous nucleation is often dendritic, then terraced, before stable facets are established.

(iii) Crystals grown in a stable mode from high-temperature solution normally have atomically flat faces, on which growth occurs by the spreading of layers from active centres. The evidence for this statement is based on observations of growth spirals and layers and it also explains the observation that crystals preserve their shape although the supersaturation is not constant across a face.

(iv) A complete description of the growth process should include desolvation and surface diffusion of solute.

(v) In unstirred solutions, volume diffusion is the most probable rate determining step. At low supersaturations screw-dislocation growth can account for most of the experimental measurements of growth kinetics although alternative explanations are often possible. The theory of solution growth is still not quantitative since it contains several parameters which cannot be determined.

(vi) No strict generalization on the growth mechanism and the rate determining step is possible. Depending on the solute-solvent system and on the experimental parameters (supersaturation, temperature, concentration, stirring, impurity concentration, etc.) each crystal will have its individual growth history.

References

- Alexandru, H. V. (1971) *J. Crystal Growth* **10**, 151.
 Amelinckx, S. (1953) *Phil. Mag.* **44**, 337.
 Amelinckx, S., Bontinck, W. and Dekeyser, W. (1957) *Phil. Mag.* **2**, 1264.
 Becke, F. (1911) *Fortschr. Min.* **1**, 68.
 Becker, R. and Döring, W. (1935) *Ann. Phys.* **24**, 719.
 Belyutsin, A. V. and Dvorykin, V. F. (1957) *Growth of Crystals* (A. V. Shubnikov and N. N. Sheftal, eds.) **1**, 139.
 Bennema, P. (1965), Thesis, University of Delft.
 Bennema, P. (1966) *phys. stat. solidi* **17**, 563.
 Bennema, P. (1967) *J. Crystal Growth* **1**, 278, 287.
 Bennema, P. (1969) *J. Crystal Growth* **5**, 29.
 Bennema, P. and Gilmer, G. H. (1972) *J. Crystal Growth* **13/14**, 148.
 Bennema, P. and Gilmer, G. H. (1973) In "Crystal Growth" (P. Hartman, ed.) North Holland, Amsterdam.
 Bennema, P. and van Rosmalen, R. (1972) *Growth of Crystals* (to be published).
 Bennema, P., Boon, J. and van Leeuwen, C. (1972) Chisa Conference Report, Prague.
 Berg, W. F. (1938) *Proc. Roy. Soc. A* **164**, 79.
 Berthoud, A. (1912) *J. Chim. Phys.* **10**, 624.
 Binsbergen, F. L. (1972) *J. Crystal Growth* **13/14**, 44.

- Boscher, J. (1965) *Ann. Assoc. Int. Calc. Analog.* **4**, 117.
- Bransom, S. H., Dunning, W. J. and Millard, B. (1949) *Disc. Faraday Soc.* **5**, 83.
- Brice, J. C. (1967) *J. Crystal Growth* **1**, 161.
- Bunn, C. W. (1949) *Disc. Faraday Soc.* **5**, 144.
- Bunn, C. W. and Emmett, H. (1949) *Disc. Faraday Soc.* **5**, 119.
- Burton, W. K. and Cabrera, N. (1949) *Disc. Faraday Soc.* **5**, 33.
- Burton, W. K., Cabrera, N. and Frank, F. C. (1951) *Phil. Trans. A* **243**, 299.
- Burton, J. A., Prim, R. C. and Slichter, W. P. (1953) *J. Chem. Phys.* **21**, 1987.
- Cabrera, N. and Coleman, R. V. (1963) In "The Art and Science of Growing Crystals" (J. J. Gilman, ed.) p. 3. Wiley, New York.
- Cabrera, N. and Levine, M. M. (1956) *Phil. Mag.* **1**, 450.
- Cabrera, N. and Vermilyea, D. A. (1958) In "Growth and Perfection of Crystals" (R. H. Doremus, B. W. Roberts, D. Turnbull, eds.) p. 393. Wiley, New York and Chapman and Hall, London.
- Carlson, A. E. (1958), Thesis, Univ. of Utah; in "Growth and Perfection of Crystals" (R. H. Doremus, B. W. Roberts, D. Turnbull, eds) p. 421. Wiley, New York and Chapman and Hall, London.
- Cartier, R., Pindola, D. and Bruins, P. (1959) *Trans. Inst. Chem. Engrs.* **51**, 1409.
- Chase, A. B. (1968) *J. Am. Ceram. Soc.* **51**, 507.
- Chase, A. B. (1971) In "Preparation and Properties of Solid State Materials" (R. A. Lefever, ed.) p. 183. Dekker, New York.
- Chernov, A. A. (1961) *Sov. Phys. Usp.* **4**, 129.
- Chernov, A. A. (1963) *Sov. Phys. Cryst.* **8**, 63.
- Cobb, C. M. and Wallis, E. B. (1967) Report AD 655388.
- Conway, B. E. and Bockris, J. O. M. (1958) *Proc. Roy. Soc. A* **248**, 394.
- Cook, C. F. and Nye, W. F. (1967) *Mat. Res. Bull.* **2**, 1.
- Coulson, J. M. and Richardson, J. F. (1956) In "Chemical Engineering" Vol. 2. Pergamon Press, Oxford.
- Davies, C. W. and Jones, A. L. (1951) *Trans. Faraday Soc.* **55**, 312.
- Dawson, R. D., Elwell, D. and Brice, J. C. (1974) *J. Crystal Growth* **23**, 65.
- Doremus, R. H. (1958) *J. Phys. Chem.* **62**, 1068.
- Dunning, W. J. (1955) In "Chemistry of the Solid State" (W. E. Garner, ed.) p. 159. Butterworth, London.
- Elwell, D. and Dawson, R. D. (1972) *J. Crystal Growth* **13/14**, 555.
- Elwell, D. and Neate, B. W. (1971) *J. Mat. Sci.* **6**, 1499.
- Elwell, D., Neate, B. W. and Smith, S. H. (1969) *J. Thermal Anal.* **1**, 319.
- Faust, Jr., J. W. and John, H. F. (1964) *J. Phys. Chem. Solids* **25**, 1407.
- Forty, A. J. (1951) *Phil. Mag.* **42**, 670.
- Frank, F. C. (1949) *Disc. Faraday Soc.* **5**, 48.
- Frank, F. C. (1958a) In "Growth and Perfection of Crystals" (R. H. Doremus, B. W. Roberts, D. Turnbull, eds.) p. 393. Wiley, New York and Chapman and Hall, London.
- Frank, F. C. (1958b) In "Growth and Perfection of Crystals" (R. H. Doremus, B. W. Roberts, D. Turnbull, eds.) p. 411. Wiley, New York and Chapman and Hall, London.
- Garabedian, H. and Strickland-Constable, R. F. (1970). Paper presented at BAGG Meeting, University of Bristol.
- Geller, S. and Bala, V. B. (1956) *Acta Cryst.* **9**, 1019.
- Gilmer, G. H. and Bennema, P. (1972) *J. Appl. Phys.* **43**, 1347.
- Gilmer, G. H., Ghez, R. and Cabrera, N. (1971) *J. Crystal Growth* **8**, 79.

- Glasner, A. (1973) *Mat. Res. Bull.* **8**, 413.
- Goldsztaub, S., Itti, R. and Mussard, F. (1970) *J. Crystal Growth* **6**, 130.
- Griffin, L. J. (1951) *Phil. Mag.* **41**, 1337.
- Hartman, P. (1956) *Acta Cryst.* **9**, 721.
- Hartman, P. and Perdok, W. G. (1955) *Acta Cryst.* **8**, 49.
- Hirth, J. P. and Pound, G. M. (1963) "Condensation and Evaporation, Nucleation and Growth Kinetics" Pergamon, Oxford.
- Hixson, A. W. and Knox, K. L. (1951) *Ind. Eng. Chem.* **43**, 2144.
- Honigmann, B. (1958) "Gleichgewichts- und Wachstumsformen von Kristallen" Steinkopff, Darmstadt.
- Jackson, K. A. (1958) In "Liquid Metals and Solidification" p. 174. Am. Soc. Metals, Cleveland.
- John, H. F. and Faust, Jr., J. W. (1961) In "Metallurgy of Elemental and Compound Semiconductors" (R. Gruebel, ed.) Interscience, New York.
- Khamskii, E. V. (1969) "Crystallization from Solutions" Consultants Bureau, New York.
- Kossel, W. (1927) *Nachr. Gesell. Wiss. Göttingen, Math-Phys. Kl.*, 135.
- Kunisaki, J. (1957) *J. Chem. Soc. Japan* **60**, 987.
- Laudise, R. A., Linares, R. C. and Dearborn, E. F. (1962) *J. Appl. Phys.* **33S**, 1362.
- Lefever, R. A. and Chase, A. B. (1962) *J. Am. Ceram. Soc.* **45**, 32.
- Lefever, R. A. and Giess, E. A. (1963) *J. Am. Ceram. Soc.* **46**, 143.
- Lewis, B. (1974) *J. Crystal Growth* **21**, 29, 40.
- Lighthill, M. J. and Whitham, G. B. (1955) *Proc. Roy. Soc.* **229**, 281.
- Lothe, J. and Pound, G. M. (1962) *J. Chem. Phys.* **36**, 2080.
- Lydin, H. (1970) "Chemical Vapour Deposition" (J. M. Blocher and J. C. Withers, eds.) 2nd Int. Conf. Electrochem. Soc., 1971.
- McCabe, W. L. and Stevens, R. P. (1951) *Chem. Eng. Progr.* **47**, 168.
- Mügge, O. (1911) *Fortschr. d. Mineral.* **1**, 38.
- Mullin, J. W. and Amatavivadhana, A. (1967) *J. Appl. Chem.* **17**, 151.
- Mullin, J. W. and Garside, J. (1967) *Trans. Inst. Chem. Engrs.* **45**, T285.
- Mullin, J. W. and Gaska, G. (1969) *Can. J. Chem. Eng.* **47**, 483.
- Nabarro, F. R. N. (1967) "Theory of Crystal Dislocations", Oxford University Press.
- Nernst, W. (1904) *Z. Phys. Chem.* **47**, 52.
- Newkirk, H. W. and Smith, D. K. (1965) *Am. Min.* **50**, 44.
- Nielsen, A. E. (1964) "Kinetics of Precipitation" Pergamon Press, Oxford.
- Nielsen, A. E. (1969) *Kristall u. Technik* **4**, 17.
- Niggli, P. (1920) In "Lehrb. d. Mineral." p. 142. Borntraeger, Berlin.
- Noyes, A. A. and Whitney, W. R. (1897) *J. Am. Chem. Soc.* **19**, 930.
- Onsager, L. (1944) *Phys. Rev.* **55**, 117.
- Parker, R. L. (1970) *Solid State Physics* (M. Ehrenreich, F. Seitz and D. Turnbull, eds.) **25**, 152.
- Quon, H. and Sadler, A. G. (1967) *J. Can. Ceram. Soc.* **36**, 33.
- Reich, R. and Kahlweit, M. (1968) *Ber. Bunseng. Phys. Chem.* **72**, 66.
- Rumford, F. and Bain, J. (1960) *Trans. Inst. Chem. Engrs.* **38**, 10.
- Scheel, H. J. and Elwell, D. (1972) *J. Crystal Growth* **12**, 153.
- Scheel, H. J. and Elwell, D. (1973a) *J. Electrochem. Soc.* **120**, 818.
- Scheel, H. J. and Elwell, D. (1973b) *J. Crystal Growth* **20**, 259.
- Scheel, H. J. and Schulz-DuBois, E. O. (1971) *J. Crystal Growth* **8**, 304.
- Seeger, A. (1953) *Phil. Mag.* **44**, 1.

- Smythe, B. M. (1967) *Austr. J. Chem.* **20**, 1087.
- Spangenberg, K. (1934) *Handb. der Naturwiss.* 2nd Edition, **10**, 362.
- Stranski, I. N. (1928) *Z. Phys. Chem.* **136**, 259.
- Strickland-Constable, R. F. (1968) "Kinetics and Mechanism of Crystallization"
Academic Press, London, New York.
- Sunagawa, I. (1960) *Mineral Journ.* **3**, 59.
- Sunagawa, I. (1967) *J. Crystal Growth* **1**, 102.
- Tammann, G. (1925) "States of Aggregation" Van Nostrand, New York.
- Ten-kin, D. E. (1966) "Crystallization Processes" p. 15. Consultants Bureau,
New York.
- Tiller, W. A. (1971) Comment at ICCG3 (Marseille).
- Tolksdorf, W. and Welz, A. (1972) *J. Crystal Growth* **13**, 566.
- Torgeson, J. L. and Jackson, R. W. (1965) *Science* **148**, 952.
- Valeton, J. J. P. (1924) *Z. Krist.* **59**, 135 and 335.
- Van Hook, A. (1945) *Ind. Eng. Chem.* **37**, 782.
- Verma, A. R. (1953) "Crystal Growth and Dislocations" Butterworth, London.
- Volmer, M. and Weber, A. (1926) *Z. Phys. Chem.* **119**, 277.
- Wagner, R. S. (1960) *Acta Met.* **8**, 51.
- Whiffin, P. A. C. and Brice, J. C. (1974) *J. Crystal Growth* **23**, 25.
- White, E. A. D. (1965) *Tech. Inorg. Chem.* **4**, 31.
- Wilcox, W. R. (1969) *Mat. Res. Bull.* **4**, 265.
- Wilcox, W. R. (1972) *J. Crystal Growth* **12**, 93.
- Zettlemoyer, A. C. (1969) (editor) "Nucleation" Dekker, New York.